

Meson-loop contributions to the ρ - ω mass splitting & ρ charge radius

M. A. Pichowsky,^{1,2} Sameer Walawalkar¹ and Simon Capstick¹

¹*Department of Physics & Supercomputer Computations Research Institute,
Florida State University, Tallahassee, FL 32306, USA*

²*Nuclear Theory Center, Indiana University, Bloomington, IN 47405, USA*

(June 22, 2021)

Contributions of two-pseudoscalar and vector-pseudoscalar meson loops to the ρ - ω mass splitting are evaluated in a covariant model based on studies of the Schwinger-Dyson equations of QCD. The role and importance of the different time orderings of the meson loops is analyzed and compared with those obtained within time-ordered perturbation theory. It is shown that each meson loop contributes less than 10% of the bare mass, and decreases as the masses of the intermediate mesons increase beyond approximately $m_\rho/2$. A mass splitting of $m_\omega - m_\rho \approx 25$ MeV is obtained from the $\pi\pi$, $K\bar{K}$, $\omega\pi$, $\rho\pi$, $\omega\eta$, $\rho\eta$ and K^*K channels. The model is then used to determine the effect of the two-pion loop on the ρ -meson electromagnetic form factor. It is shown that the inclusion of pion loops increases the ρ -meson charge radius by 10%.

I. INTRODUCTION

In a fully-interacting theory, the number of constituents of a hadron is not conserved, and the picture of a hadron as being comprised of three quarks (baryon) or a quark and antiquark (meson) is naïve. One way to go beyond a picture in which hadrons are simple bound states of valence quarks is to consider their mixing with multiple-hadron states. The success of models which describe hadrons in terms of only a few degrees of freedom, such as the constituent-quark model, suggests that mixing with multiple-hadron states should represent only a small correction to the predominant valence quark structure of the hadron.

Some observables may be sensitive to contributions that arise from mixings of hadrons with multiple-hadron states. These observables would provide a means to probe the structure of hadrons beyond that of the valence quarks. One such observable is the mass splitting between the ρ and ω mesons, which is the subject of this article.

The ρ^0 and ω have a similar quark substructure, differing only in their total isospin (and hence G -parity). SU(3)-flavor violating contributions due to the different masses of the u , d and s quarks tend to split the masses of the ρ and ω mesons. However, these contributions alone do not account for most of the mass splitting [1]. Other contributions arise from the mixing of the ρ and ω mesons with multiple-hadron states of differing G -parity. An important example of this is the shift in the mass of the ρ meson due to its mixing with the two-pion state. As mixing between the ω meson and the two-pion state is forbidden by G -parity, the mass of the ω meson doesn't receive such a contribution from the two-pion state. The difference between the ρ and ω mesons due to mixing with all possible multiple-hadron states results in an ob-

servable splitting of the masses m_ρ and m_ω , which would otherwise be degenerate (in the absence of SU(3)-flavor breaking).

In Ref. [2], the mass shift of the ρ meson due to its mixing with the two-pion state was investigated using an effective chiral Lagrangian approach. A form factor was introduced into the resulting dispersion relations for the ρ -meson self energy $\Pi_{\mu\nu}(q^2)$ to render it finite. Several different forms of this form factor were considered and each produced similar results. For example, using a dipole form factor, it was found, over a large range of dipole widths $0.6 \leq \Lambda^2 \leq 4.0$ GeV², that the ρ -meson mass is shifted by roughly -10 to -20 MeV due to its coupling with the two-pion state.

The purpose of the study of Ref. [2] was to determine whether results obtained by lattice studies of QCD for the ρ meson mass are significantly affected when the ρ meson is “unquenched”; that is, when the ρ meson is allowed to mix with two-pion states. Such mixings with multiple-hadron states are typically neglected in lattice studies. It is clear from the study, which relies on very little dynamical modeling, that the inclusion of intermediate meson states into the vector-meson self energy $\Pi_{\mu\nu}(q^2)$ is indeed a small effect which can be treated as a correction to the predominant quark-antiquark structure of the vector meson.

An extensive study of the ρ - ω mass splitting is carried out in Ref. [3]. In this work the contributions of many different two-meson intermediate states to the masses of the ρ and ω are evaluated within a nonrelativistic framework, using time-ordered perturbation theory to evaluate the loops. The three-meson vertices and their momentum dependence are evaluated using a string-breaking picture of the strong decays based on the flux-tube model of the confining interaction, and quark pair creation with vacuum (3P_0) quantum numbers. It is noted that the ρ - ω

splitting is directly proportional to an OZI-violating mixing between ground-state vector $u\bar{u}$ and $d\bar{d}$ mesons. This mixing is due to two-meson intermediate states which can link the initial and final mesons. It is shown in Ref. [3] that, in the closure limit where the energy denominators for the intermediate states are constant, the 3P_0 pair-creation operator cannot link these two vector states, so that the OZI rule is exact in this limit. The presence of a small OZI-violating mass splitting is, therefore, interpreted as a deviation of the sum over intermediate states from this closure limit due to the differing properties of the physical intermediate states.

Although the authors of Ref. [3] point out that their calculation of this mixing is not formally complete due to the absence of pure annihilation diagrams where the intermediate state contains only glue (which can be written as a sum over heavier glueball states and are likely suppressed), the sum over intermediate states is much more extensive than that carried out here. The convergence of this sum, although convincingly demonstrated, is rather slow in their calculation, requiring many different meson pairs with many possible relative angular momenta. This can be illustrated by examining the size of individual terms in the sum; for example, the $\pi\pi$ loop contributes -142 MeV to the ρ mass, and the $\omega\pi$ loop contributes -146 MeV (the corresponding $\rho\pi$ loop contributes roughly three times this amount to the ω mass). It is pointed out in Ref. [3] that without a flux-tube overlap function and a form factor at the pair creation vertex, both of which are necessary for a theoretically consistent picture of the strong decays and suppress high-momentum created pairs, this sum would not formally converge. Note that neither of these features of the strong decay model are essential to fitting the strong decays of mesons in this picture, but were essential to the convergence of the loop expansion in Ref. [3]. A global fit to the meson decays was carried out in order to fit the decay model (in particular the pair creation vertex form factor).

It was concluded in Ref. [3] that reasonable results for the ρ - ω mass splitting could be obtained only when the effects of many two-meson intermediate states are included in the loop expansion. Such a conclusion raises questions about the validity of the usual picture of a meson as being well described as a bound state of a valence quark and antiquark.

The motivation for carrying out the present study is to attempt to reconcile the small effects on the ρ mass due to the two-pion loop found in Ref. [2] with the more substantial mass shift found in Ref. [3], and to examine the consequences for the convergence of the sum over intermediate states performed in Ref. [3]. The ρ - ω mass splitting is evaluated using meson transition form factors obtained from a covariant, quantum field theoretic model based on the Schwinger-Dyson equations of QCD. A similar approach was employed in Ref. [1] for the $\pi\pi$ intermediate state. The present study extends the work of Refs. [1,2] by considering the additional channels $K\bar{K}$,

$\omega\pi$, $\rho\pi$, $\omega\eta$, $\rho\eta$, and K^*K . (In Ref. [4], a non-local quark four-point interaction was used to study the ρ - ω mass splitting and it was shown that the three-meson intermediate state $\pi\pi\pi$ produces a negligible mass shift. Hence, three-meson intermediate states are neglected in the present study.) The model employed is fit to various properties and electromagnetic form factors of the π and K , and has been shown to give reasonable results for the decays and electromagnetic form factors of the light vector mesons in Ref. [5].

Although a very different framework is employed here, results that are qualitatively and quantitatively similar to those found in Refs. [2] are obtained for the ρ -meson mass shift due to the two-pion loop. In each of the seven channels considered here, a mass shift of less than 10% of the total mass of the ρ is observed. These mass shifts partially cancel each other when calculating the difference $m_\omega - m_\rho$, as observed in Ref. [3], and we obtain a net mass splitting of $m_\omega - m_\rho \approx 25$ MeV. The experimentally observed value for this mass splitting is $m_\omega - m_\rho = 12 \pm 1$ MeV.

Of course, the calculation of the ρ - ω mass splitting described herein is incomplete. Other channels, such as the two-vector-meson intermediate states, might be expected to contribute significantly [3]. Nonetheless, these results are consistent with those obtained in Ref. [2], and indicate that the sum over two-meson intermediate states should converge quite rapidly as the masses of the intermediate state mesons increase, in contrast to what is found in Ref. [3].

The dependence of the vector meson self energy on the masses of the intermediate mesons is also explored in detail. It is shown that contributions from two-meson loops with meson masses above $m_\rho/2$ contribute only small amounts to the mass shift, and their contributions decrease rapidly as the masses of the intermediate mesons are increased. This is the essential mechanism for the expected rapid convergence of the sum over two-meson loops and is insensitive to the details of the model meson transition form factors, the only dynamical input employed in the present calculations.

Another observable that is sensitive to the inclusion of meson loops is also explored in this study for the first time. With the same $\rho \rightarrow \pi\pi$ transition form factors used in the calculation of the ρ - ω mass splitting, the contribution of $\pi\pi$ loops to the ρ -meson electromagnetic form factor is calculated. This model predicts a 10% increase in the charge radius of the ρ meson relative to that obtained in Ref. [5] which considered only the quark-antiquark structure of the vector meson. The inclusion of pion loops leads to a similar 10–15% increase for the π -meson charge radius [6]. The results from the present study also indicate that of the two-meson states considered, the two-pion state provides the most significant correction to the vector meson charge radius.

The brief lifetime of the ρ meson makes a direct measurement of its electromagnetic charge radius impossible at present. However, the size of the neutral vector me-

son can be extracted from high-energy data for diffractive, vector meson photoproduction on a nucleon. It is possible, using a semi-empirical model of diffractive photoproduction [7], to relate the *diffractive radii* of mesons to their charge radii. Given the dominance of the two-pion state this implies that the increase in the charge radius of the ρ meson due to the two-pion loop corresponds to an analogous increase of the diffractive radius of the ρ meson. Since G -parity forbids the ω meson from receiving such contributions from the two-pion state, a measured difference in the diffractive radii of the ρ and ω mesons can provide a means to probe the magnitude of the two-pion contribution to ρ meson observables.

The organization of this article is as follows. In Sec. II A, the general Lorentz and flavor structure of the meson transition amplitudes, necessary for the calculation of the vector-meson self energy and electromagnetic form factors, are derived. These elements are then employed in a study of the Schwinger-Dyson equation for the vector meson propagator in Sec. II B. The mass of the vector meson is related to the real part of the vector-meson self energy, and the total decay width of the vector meson is related to the imaginary part. These same elements are then employed in a study of the ρ meson electromagnetic form factors in Sec. II C.

In Sec. III, the contributions to the vector-meson self energy arising for the different time orderings of the intermediate meson propagators are investigated. Aspects of time-ordered quantum mechanical frameworks, such as that employed in Ref. [3], and the Lorentz-covariant Euclidean-based quantum field theoretic framework employed here are discussed and contrasted.

In Sec. IV, the dynamical model used to calculate the off-mass-shell behavior of the meson transition amplitudes is described. The model describes the meson transitions in terms of loops involving nonperturbatively-dressed quarks and model Bethe-Salpeter amplitudes that describe the quark-antiquark substructure of the mesons. The dressed-quark propagators and Bethe-Salpeter amplitudes employed herein were developed and tested in numerous studies of meson observables [5,8,9] and in numerical studies of the quark Schwinger-Dyson equation of QCD [10–12].

Results for the ρ - and ω -meson self energies are given in Secs. V A and V B. In Sec. V C, numerical results for each of the possible time orderings of the two-pion-loop contribution to the self energy are provided. Results for ρ -meson electromagnetic form factor G_E and charge radius are given in Sec. V D. The conclusions of this study are given in Sec. VI.

II. MESON-LOOP CONTRIBUTIONS

In this section some of the formalism necessary to describe the effects of two-meson loops on the vector-meson self energy and electromagnetic form factors is presented.

In Sec. II A, the most general Lorentz-, parity- and SU(3)-flavor-covariant amplitudes that describe the coupling of a vector meson to two pseudoscalar mesons or a vector and a pseudoscalar meson are presented. The transition amplitudes are written in terms of a coupling constant and an *off-mass-shell* transition form factor. Both are defined so that the transition form factor is equal to one when all three mesons are on shell. In the case of the ρ meson coupling to two pions, the coupling constant associated with the transition amplitude is related to the decay $\rho \rightarrow \pi\pi$ and is found by experiment to be $g_{\rho\pi\pi} = 6.03$. The other coupling constants considered herein as well as the off-mass-shell transition form factors are obtained from considerations of SU(3)-flavor invariance or the dynamical model described in Sec. IV.

In Sec. II B, the Schwinger-Dyson equation for the vector meson propagator is given in terms of the vector meson self energy $\Pi_{\mu\nu}(q)$. Expressions are derived that give the self energy in terms of loop integrations involving the propagators for the two intermediate mesons and the transition amplitudes described in Sec. II A. The imaginary part of the vector-meson self energy is related to the total decay width of the vector meson, and the real part of the self energy provides a contribution to the vector meson mass.

In Sec. II C, the contribution of the two-pion loop to the ρ -meson electromagnetic form factors is considered. A correction to the electromagnetic (EM) charge radius of the ρ meson due to pion loops is obtained, and is compared to the results obtained from a study of the quark-antiquark contribution from Ref. [5]. It is argued that since G -parity forbids the ω meson coupling to two pions, and since the two-pion contribution dominates, measurement of the difference of the ρ meson and ω meson charge radii provides a means to determine the effects of including such intermediate meson loops. The electromagnetic form factors are given in terms of the same meson transition amplitudes used in Sec. II B to calculate the self energies and decay width of the ρ meson. Hence, the calculation of the contribution of pion loops to the ρ meson EM form factor provides a further test of the self-consistency of the present approach.

A. Meson transition amplitudes

The most general coupling of a ρ meson to two pseudoscalar mesons (π or K) can be written in terms of the following action:

$$S = \int d^4x d^4y d^4z \pi^i(x) \pi^j(y) \rho_\mu^k(z) \Lambda_\mu^{ijk}(x-z, y-z), \quad (2.1)$$

where $\rho_\mu^k(z)$ is the ρ meson field with flavor index k and Lorentz index μ , and $\pi^i(x)$ is the pseudoscalar meson field with flavor i . The nonlocal three-point coupling is described by the amplitude

$$\Lambda_\mu^{ijk}(x-z, y-z) = \int \frac{d^4 p_1}{(2\pi)^4} \frac{d^4 p_2}{(2\pi)^4} e^{-ip_1(x-z) - ip_2(y-z)} \Lambda_\mu^{ijk}(p_1, p_2), \quad (2.2)$$

which can be written in terms of a coupling constant g_{ijk} , where i, j , and k are SU(3)-flavor indices, and a form factor $f^{VPP}(p_1, p_2)$ which is a function of the Lorentz invariants p_1^2, p_2^2 and $q^2 = (p_1 + p_2)^2$. The form factor $f^{VPP}(p_1, p_2)$ is defined to be equal to unity, when all three mesons are on their mass shell; that is, $f^{VPP}(p_1, p_2) = 1$ when $p_1^2 = p_2^2 = -m_\pi^2, q^2 = (p_1 + p_2)^2 = -m_\rho^2$. Hence, one may write:

$$\Lambda_\mu^{ijk}(p_1, p_2) = \frac{1}{2}(p_1 - p_2)_\mu g^{ijk} f^{VPP}(p_1, p_2). \quad (2.3)$$

In general, Eq. (2.3) may also have a term which is proportional to $(p_1 + p_2)_\mu$. Even if such a term were present, it could not contribute to the self energy of an *on-shell* vector meson since its contraction with a spin-1 polarization vector is zero. For $\rho \rightarrow \pi\pi$, $g^{ijk} \equiv g_{\rho\pi\pi} \epsilon^{ijk}$.

From the above amplitude, one obtains the invariant Feynman amplitude for the decay of, say, the ρ^0 into two charged pions:

$$\begin{aligned} & \langle \pi^+(p_1); \pi^-(p_2) | T | \rho^0(q, \lambda) \rangle \\ &= \varepsilon_\mu(q, \lambda) [\Lambda_\mu^{-+3}(p_1, p_2) + \Lambda_\mu^{+-3}(p_2, p_1)], \end{aligned} \quad (2.4)$$

$$= 2g_{\rho\pi\pi} p_1 \cdot \varepsilon(q, \lambda), \quad (2.5)$$

where $\varepsilon_\mu(q, \lambda)$ is the polarization vector for a ρ meson of momentum q and helicity λ . The resulting $\rho \rightarrow \pi\pi$ decay width is

$$\Gamma_{\rho \rightarrow \pi\pi} = \frac{g_{\rho\pi\pi}^2}{4\pi} \frac{m_\rho}{12} \left[1 - \frac{4m_\pi^2}{m_\rho^2} \right]^{3/2}. \quad (2.6)$$

The meson transition form factor $f^{VPP}(p_1, p_2)$ does not appear in the relation for the decay width because it is unity when all mesons are on their mass shell. Its value away from this point is therefore not directly observable and must be calculated from a dynamical model.

Similarly, the coupling of an ω meson to a ρ and π meson is described by the action:

$$S = \int d^4x d^4y d^4z \rho_\mu^i(x) \pi^j(y) \omega_\nu(z) \Lambda_{\mu\nu}^{ij}(x-z, y-z). \quad (2.7)$$

Here, $\omega_\nu(z)$ is the ω -meson field and $\Lambda_{\mu\nu}^{ij}(x-z, y-z)$ is the nonlocal transition amplitude describing the coupling of two vector mesons to a pseudoscalar meson. Introducing the coupling constant $g_{\omega\rho\pi}$ and form factor $f^{VVP}(p_1, p_2)$, considerations of Lorentz covariance give the Fourier transform of $\Lambda_{\mu\nu}^{ij}(x-z, y-z)$ as

$$\Lambda_{\mu\nu}^{ij}(p_1, p_2) = \epsilon_{\mu\nu\alpha\beta} \frac{p_{1\alpha} p_{2\beta}}{m_\rho} \delta^{ij} g_{\omega\rho\pi} f^{VVP}(p_1, p_2) \quad (2.8)$$

where p_1 and p_2 are the momenta of the ρ and π mesons, respectively, and $f^{VVP}(p_1, p_2) = 1$ when $q^2 = (p_1 +$

$p_2)^2 = -m_\omega^2, p_1^2 = -m_\rho^2$, and $p_2^2 = -m_\pi^2$. Unlike the previous case, a lack of phase space prevents the decay $\omega \rightarrow \rho\pi$, so that it is impossible to determine the value of the coupling constant $g_{\omega\rho\pi}$ from experiment. Hence, both the meson-transition form factor $f^{VVP}(p_1, p_2)$ and the coupling constant $g_{\omega\rho\pi}$ must be determined from a model calculation.

In Sec. IV, a dynamical model is described and used to determine the transition form factors $f^{VPP}(p_1, p_2)$ and $f^{VVP}(p_1, p_2)$, and the coupling constant $g_{\omega\rho\pi}$. The model has been shown to give good results for the similar, physically accessible decays $\rho \rightarrow \pi\gamma$ and $K^* \rightarrow K\gamma$, in which a vector meson decays into a vector and pseudoscalar [5]. The value of the coupling constant $g_{\rho\pi\pi} = 6.03$ used herein is extracted from the experimentally observable $\rho \rightarrow \pi\pi$ decay width using Eq. (2.6).

B. Vector-meson self energy

The spin-1 nature of a vector meson entails the following form for the vector-meson self energy when the vector meson is on mass shell ($q^2 = -m_V^2$):

$$\Pi_{\mu\nu}(q) = \left(\delta_{\mu\nu} - \frac{q_\mu q_\nu}{q^2} \right) \Pi(q^2) \quad (2.9)$$

Away from the on-mass-shell point $q^2 = -m_V^2$, the vector-meson self energy is of the general form:

$$\Pi_{\mu\nu}(q) = \left(\delta_{\mu\nu} - \frac{q_\mu q_\nu}{q^2} \right) \Pi(q^2) + \frac{q_\mu q_\nu}{q^2} \Theta(q^2). \quad (2.10)$$

To project out the Lorentz scalar function $\Pi(q^2)$, a projection operator $\frac{1}{3} \mathbf{T}_{\mu\nu}(q, q^2)$ where

$$\mathbf{T}_{\mu\nu}(q, -m^2) \equiv \delta_{\mu\nu} + q_\mu q_\nu / m^2. \quad (2.11)$$

is employed.

In the following, the dressed vector meson propagator $\tilde{D}_{\mu\nu}(q) = \mathbf{T}_{\mu\nu}(q, -m_V^2) \tilde{D}(q^2)$ is given in terms of the “bare” vector meson propagator $D_{\mu\nu}(q) = \mathbf{T}_{\mu\nu}(q, -m_V^2) D_0(q^2)$ and the vector-meson self energy $\Pi_{\mu\nu}(q) = \mathbf{T}_{\mu\nu}(q, -m_V^2) \Pi(q^2)$ which describes the mixing of the vector meson with meson loops (and in general, multiple-hadron intermediate states). The “bare” vector-meson propagator $D_0(q^2)$ is presumed to arise from the quark-antiquark structure of the vector meson, and does not include the effects of multiple-meson intermediate states. Defined in this manner, quark confinement requires that the “bare” vector-meson propagator $D_0(q^2)$ is a real-valued function of q^2 . The presence of a non-zero imaginary part for $D_0(q^2)$ would entail a loss of flux for vector-meson propagation, which is a signal for the existence of open decay channels for the vector meson. In our approach, such decay channels arise from the coupling of the vector meson with multiple-hadron states. Mixing the vector meson with multiple-hadron states results in a dressed, vector-meson propagator $\tilde{D}(q^2)$ that is

a complex-valued function of the vector-meson momentum q^2 .

The dressed, vector-meson propagator $\tilde{D}(q^2)$ is obtained by solving the Schwinger-Dyson equation:

$$\tilde{D} = D_0 + D_0 \Pi \tilde{D}. \quad (2.12)$$

This integral equation gives the dressed vector meson propagator $\tilde{D}(q^2)$ in terms of the bare propagator $D_0(q^2)$ by dressing the vector meson by two-meson loops as given by $\Pi(q^2)$. As an integral equation, Eq. (2.12) necessarily implies the insertion of infinitely many self-energy $\Pi(q^2)$ contributions into the dressed, vector-meson propagator $\tilde{D}(q^2)$; hence, the dressing of the vector-meson propagator resulting from Eq. (2.12) is inherently nonperturbative.

The solution to the Schwinger-Dyson equation is

$$\begin{aligned} \tilde{D} &= D_0 + D_0 \Pi D_0 + D_0 \Pi D_0 \Pi D_0 + \dots, \\ &= D_0 \left(\frac{1}{1 + \Pi D_0} \right), \end{aligned} \quad (2.13)$$

so that

$$\tilde{D}^{-1} = (1 + \Pi D_0) D_0^{-1} = D_0^{-1} + \Pi. \quad (2.14)$$

Near $q^2 = -m_V^2$, the difference between the dressed and bare inverse propagators is given by

$$\begin{aligned} \Pi(q^2) &= \tilde{D}^{-1}(q^2) - D_0^{-1}(q^2) \\ &= (1 + \delta Z) (q^2 + m_V^2 - im_V \Gamma) - (q^2 + m_0^2), \end{aligned} \quad (2.15)$$

where m_0 is the bare mass of the vector meson, Γ is the total decay width of the vector meson, and $1 + \delta Z$ is the field renormalization for the vector meson, chosen to ensure that the asymptotic vector meson has unit normalization. In Sec. IV, the Bethe-Salpeter amplitudes, which describe the quark-antiquark substructure of the meson, are normalized to unity. Thus, from the definition of the normalization $1 + \delta Z$, as given by Eq. (2.15), it follows that the *correction* to the normalization that results from the inclusion of meson-loops is given by δZ . For meson loops to be considered as a small effect, δZ must be smaller than one.

Comparison of Eq. (2.15) and Eq. (2.14) gives

$$-\text{Im}(\Pi) = (1 + \delta Z) m_V \Gamma \quad (2.16)$$

$$\text{Re}(\Pi) = \delta Z q^2 + (1 + \delta Z) m_V^2 - m_0^2. \quad (2.17)$$

Eq. (2.17) provides a means to determine the normalization δZ from the self energy $\Pi(q^2)$:

$$\frac{d}{dq^2} [\text{Re}\Pi(q^2)]_{q^2=-m_V^2} = \delta Z, \quad (2.18)$$

from which it follows:

$$m_V^2 = m_0^2 + \text{Re}\Pi(-m_V^2). \quad (2.19)$$

This equation gives the mass of the vector meson m_V , in terms of the bare mass m_0 (arising from the quark-antiquark substructure of the vector meson) and the self energy $\Pi(q^2)$. It can be solved iteratively,

$$\begin{aligned} m_V^2 &= m_0^2 + \text{Re}\Pi(-m_0^2 - \text{Re}\Pi(-m_V^2)) \\ &\approx m_0^2 + \text{Re}\Pi(-m_0^2) - \text{Re}\Pi'(-m_0^2) \text{Re}\Pi(-m_0^2), \end{aligned} \quad (2.20)$$

where the expansion assumes small $m_V^2 - m_0^2$. This relation yields a first-order correction to the vector meson mass:

$$m_V^2 \approx m_0^2 + \text{Re}\Pi(-m_0^2). \quad (2.21)$$

From Eq. (2.18), one identifies $\text{Re}\Pi'(-m_V^2)$ with δZ . Thus, the second order correction to the vector meson mass shift is $-\delta Z \text{Re}\Pi(-m_0^2)$, which is suppressed by a factor δZ compared to the first-order term in Eq. (2.20). The importance of higher-order corrections can be estimated from the momentum dependence of $\Pi(q^2)$ in the vicinity of m_0^2 . It is found to be sufficient (see Sec. V) to include only the lowest-order term from Eq. (2.20) to obtain a good estimate for the dressed, vector-meson mass m_V .

As stated above, the self energy $\Pi(q^2)$ describes the dressing of the vector meson due to two-meson loops. It can be described in terms of a fluctuation of the vector meson into a multiple-meson intermediate state. This is given in terms of meson transition amplitudes, the form of which was described in Sec. II A, and propagators for the intermediate mesons. The contribution to the vector-meson self energy $\Pi(q^2)$ due to a two-pseudoscalar-meson loop is then given by

$$\begin{aligned} \Pi_{\mu\nu}^{kk'}(q) &= -2 \int \frac{d^4k}{(2\pi)^4} \Lambda_{\mu}^{ijk}(-p_1, -p_2) \Delta(p_1, m_P) \\ &\quad \times \Delta(p_2, m_{P'}) \Lambda_{\nu}^{ijk'}(p_1, p_2) \\ &= \delta^{kk'} \Pi_{\mu\nu}(q), \end{aligned} \quad (2.22)$$

where m_P and $m_{P'}$ are the masses of the pseudoscalar mesons, $p_1 = \frac{1}{2}q + k$, $p_2 = \frac{1}{2}q - k$, and the meson transition amplitude $\Lambda_{\mu}^{ijk}(p_1, p_2)$, given by Eq. (2.3), describes the transition $V \rightarrow PP$ from a vector meson V to two-pseudoscalar mesons P and P with momenta p_1 and p_2 , respectively. The propagation of the intermediate pseudoscalar mesons is given in terms of the following scalar-boson propagator:

$$\Delta(p_1, m_P) = (p_1^2 + m_P^2 - i\epsilon)^{-1}, \quad (2.23)$$

where ϵ is an infinitesimal positive number included to ensure the proper boundary conditions for the decay $V \rightarrow PP$. This process is depicted in Fig. 1, in which the meson transition amplitude $\Lambda_{\mu}^{ijk}(p_1, p_2)$ is given in terms of a quark-loop triangle diagram. In Sec. IV, the transition form factor is calculated using the dressed-quark propagators and Bethe-Salpeter amplitudes of a quantum

field theoretic model based on studies of the Schwinger-Dyson equations of QCD. In impulse approximation, the leading contribution to the meson transition amplitude $\Lambda_{\mu}^{ijk}(p_1, p_2)$ is given in terms of the triangle diagram depicted in Fig. 1.

Applying the projection operator $\frac{1}{3}T_{\mu\nu}(q, q^2)$ of Eq. (2.11) to $\Pi_{\mu\nu}(q)$ in Eq. (2.22) yields the Lorentz-scalar vector meson self energy due to two-pseudoscalar-meson loops

$$\Pi^{PP}(q^2, m_P, m_{P'}) = -\frac{4}{3} \int \frac{d^4k}{(2\pi)^4} \Delta(p_1, m_P) \Delta(p_2, m_{P'}) \mathcal{F}^{PP}(k, q), \quad (2.24)$$

with

$$\mathcal{F}^{PP}(k, q) = \left(k^2 - \frac{k \cdot q^2}{q^2} \right) [g_{\rho\pi\pi} f^{VPP}(p_1, p_2)]^2. \quad (2.25)$$

Similarly, the contribution of a vector-pseudoscalar-meson loop to the vector-meson self energy is given by

$$\begin{aligned} \Pi_{\mu\nu}^{ii'}(q) &= \int \frac{d^4k}{(2\pi)^4} \Lambda_{\mu\sigma}^{ij}(-p_1, -p_2) D_{\sigma\tau}(p_1, m_V) \\ &\quad \times \Delta(p_2, m_P) \Lambda_{\nu\tau}^{i'j}(p_1, p_2), \end{aligned} \quad (2.26)$$

where m_V and m_P are the masses of the intermediate vector and pseudoscalar mesons, respectively, and the meson transition amplitude $\Lambda_{\mu\nu}^{ij}(p_1, p_2)$ is given by Eq. (2.8). The propagator for the intermediate vector meson may be written as

$$D_{\mu\nu}(p, m_V) = \left(\delta_{\mu\nu} + \frac{p_\mu p_\nu}{m_V^2} \right) \Delta(p, m_V). \quad (2.27)$$

Substituting this and the relation for $\Lambda_{\mu\nu}^{ij}(p_1, p_2)$ from Eq. (2.8) into Eq. (2.26), and applying the projection operator $\frac{1}{3}\mathbf{T}_{\mu\nu}(q, q^2)$ to the result, yields

$$\begin{aligned} \Pi^{VP}(q^2, m_V, m_P) &= \\ \frac{2}{3} \int \frac{d^4k}{(2\pi)^4} \Delta(p_1, m_V) \Delta(p_2, m_P) \mathcal{F}^{VP}(k, q), \end{aligned} \quad (2.28)$$

with

$$\mathcal{F}^{VP}(k, q) = \left[\frac{(k \cdot q)^2 - k^2 q^2}{m_\rho^2} \right] [g_{\omega\rho\pi} f^{VVP}(p_1, p_2)]^2. \quad (2.29)$$

The flavor structure of the amplitudes in Eqs. (2.22) and (2.26) are given for the particular case of the ρ meson self energy. It is easy to generalize the relations in Eqs. (2.24) and (2.28) to obtain the isoscalar ω -meson self energy. Assuming that the coupling constants for $V \rightarrow PP$ and $V \rightarrow VP$ are SU(3)-flavor symmetric, one can write the self energy of the ρ meson and the ω meson in terms of the Lorentz-scalar functions $\Pi^{PP}(q^2, m_P, m_{P'})$ and $\Pi^{VP}(q^2, m_V, m_P)$ given by

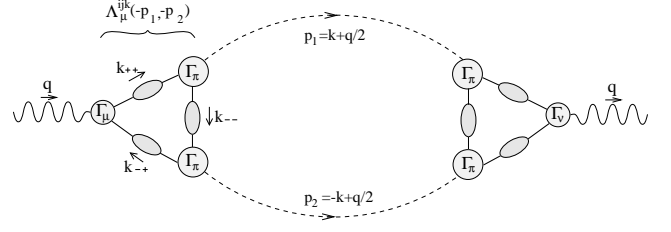


FIG. 1. Feynman diagram depicting the quark substructure of the vector-two-pseudoscalar meson transition amplitude $\Lambda_{\mu}^{ijk}(p_1, p_2)$ (shown as a triangle-shaped quark-loop diagram) given by Eq. (4.1) and the intermediate pion propagators (dashed curves) necessary for the calculation of the vector-meson self energy $\Pi^{PP}(q^2, m_P, m_P)$.

Eqs. (2.24) and (2.28), respectively, for several possible channels involving the SU(3)-octet of vector and pseudoscalar mesons. For simplicity, only those two-meson loops with the lowest mass intermediate mesons are included in the calculation of the vector-meson self energy $\Pi(q^2)$. In Sec. V, it is shown that meson loops involving mesons with higher masses are suppressed relative to those with lower masses and from Ref. [4], contributions from three-meson loops are expected to be very small. For the present study, the following channels are included: $\pi\pi$, $K\bar{K}$, $\rho\pi$, $\omega\pi$, $\rho\eta$, $\omega\eta$, and K^*K . Hence, the self energy of the ρ -meson is given by

$$\begin{aligned} \Pi(q^2) &= \Pi^{PP}(q^2, m_\pi, m_\pi) + \frac{1}{2}\Pi^{PP}(q^2, m_K, m_K) \\ &\quad + \Pi^{VP}(q^2, m_\omega, m_\pi) + \Pi^{VP}(q^2, m_{K^*}, m_K) \\ &\quad + \Pi^{VP}(q^2, m_\rho, m_\eta), \end{aligned} \quad (2.30)$$

and that of the ω meson is given by

$$\begin{aligned} \Pi(q^2) &= 0 + \frac{1}{2}\Pi^{PP}(q^2, m_K, m_K) \\ &\quad + 3\Pi^{VP}(q^2, m_\rho, m_\pi) + \Pi^{VP}(q^2, m_{K^*}, m_K) \\ &\quad + \Pi^{VP}(q^2, m_\omega, m_\eta). \end{aligned} \quad (2.31)$$

Once the meson transition form factors have been determined from a dynamical model, the contributions of the self energies can be obtained from Eqs. (2.30) and (2.31) in a straight-forward manner.

As an example, consider the calculation of the loop integral necessary to obtain $\Pi^{PP}(q^2)$, which is illustrated in Fig. 1 and is given by Eqs. (2.24) and (2.25),

$$\begin{aligned} \Pi^{PP}(q^2, m_P, m_{P'}) &= -\frac{4}{3} \int \frac{d^4k}{(2\pi)^4} \\ &\quad \frac{\mathcal{F}^{PP}(k, q)}{[(k + q/2)^2 + m_P^2 - i\epsilon][(k - q/2)^2 + m_{P'}^2 - i\epsilon]}. \end{aligned} \quad (2.32)$$

Introducing a Feynman parametrization

$$\frac{1}{a_1 a_2} = \int_0^1 \frac{dx}{[(a_1 - a_2)x + a_2]^2}, \quad (2.33)$$

the denominators of the propagators in Eq. (2.32) can be combined. With a change in variables $k \rightarrow k + \alpha q$, where

$\alpha = x - 1/2$, two of the integrations can be performed trivially, giving

$$\begin{aligned} & \Pi^{PP}(q^2, m_P, m_{P'}) \\ &= -\frac{4}{3} \int_{-\frac{1}{2}}^{\frac{1}{2}} d\alpha \int \frac{d^4k}{(2\pi)^4} \frac{\mathcal{F}^{PP}(k - \alpha q, q)}{[k^2 - (\alpha^2 - \frac{1}{4})q^2 + \bar{m}^2 + \alpha\tilde{m}^2 - i\epsilon]^2}, \\ &= -\frac{4}{3} \frac{1}{(2\pi)^3} \int_{-\frac{1}{2}}^{\frac{1}{2}} d\alpha \int_{-1}^1 dz \sqrt{1 - z^2} \\ & \quad \times \int_0^\infty k^2 dk^2 \frac{\mathcal{F}^{PP}(k - \alpha q, q)}{[k^2 - (\alpha^2 - \frac{1}{4})q^2 + \bar{m}^2 + \alpha\tilde{m}^2 - i\epsilon]^2}, \quad (2.34) \end{aligned}$$

where z is the cosine of the angle between k and q , defined by $k \cdot q = \sqrt{k^2} \sqrt{q^2} z$, $\bar{m}^2 = \frac{1}{2}(m_P^2 + m_{P'}^2)$ and $\tilde{m}^2 = (m_P^2 - m_{P'}^2)$. An inspection of Eq. (2.34) reveals that the denominator exhibits a zero in the limit that $\epsilon \rightarrow 0$ for k^2 equal to

$$k_0^2 = (\alpha^2 - \frac{1}{4})q^2 - \bar{m}^2 - \alpha\tilde{m}^2. \quad (2.35)$$

This singular behavior leads to a simple pole in the vector-meson self energy that is associated with the decay of the vector meson into two pseudoscalars.

The integral in Eq. (2.34) is evaluated numerically by first eliminating one factor of the singularity using

$$\left(\frac{1}{k^2 - k_0^2} \right)^2 = \frac{d}{dk^2} \frac{-1}{k^2 - k_0^2}, \quad (2.36)$$

integrating k^2 by parts twice, and noting that Cauchy's theorem entails

$$\lim_{\epsilon \rightarrow 0^+} \frac{1}{k^2 - k_0^2 - i\epsilon} = \frac{\mathcal{P}}{k^2 - k_0^2} + i\pi\delta(k^2 - k_0^2), \quad (2.37)$$

where \mathcal{P} denotes the principal part of the integration.

The imaginary part of Eq. (2.34) is obtained quite easily. To evaluate the principal part, the k^2 -integration domain is divided into two regions. The first region is from the origin ($k^2 = 0$) to twice the distance from the pole to the origin ($2k_0^2$). The second region is from $k^2 = 2k_0^2$ to $k^2 = \infty$. The integrations are numerically calculated using the method of quadratures. In the first region of the integration over k^2 , each mesh point of the integration is paired with one that is equidistant from the pole at k_0^2 to ensure the best cancellation of round-off errors. In the second region, the integration is straight-forward. In Sec. II A, it is shown that the meson transition amplitudes $f^{VPP}(p_1, p_2)$ decrease rapidly with increasing k^2 , providing sufficient damping to the integrations in Eqs. (2.24) and (2.28) to ensure their convergence. Similar techniques are employed in the calculation of the loop integral $\Pi^{VP}(q^2, m_V, m_P)$.

C. Vector meson electromagnetic form factor

The emission or absorption of a photon by an on-mass-shell ρ meson is described by the action:

$$\begin{aligned} S &= \int d^4x d^4y d^4z \rho_\alpha^i(x) \rho_\beta^j(y) A_\mu(z) \\ & \quad \times \epsilon^{ij3} \Lambda_{\mu\alpha\beta}(x - z, y - z). \quad (2.38) \end{aligned}$$

Charge conjugation and Lorentz covariance constrain the form of the amplitude $\Lambda_{\mu\alpha\beta}(x - z, y - z)$. Its Fourier transform is written in terms of three Lorentz-invariant form factors $G_i(Q^2)$ for $i = 1, 2, 3$, which depend only on the square of the photon momentum $Q^2 = (-q - q')^2$,

$$\Lambda_{\mu\alpha\beta}(q, q') = \sum_{i=1}^3 G_i(Q^2) T_{\mu\alpha\beta}^{[i]}(q, q'), \quad (2.39)$$

where

$$\begin{aligned} T_{\mu\alpha\beta}^{[1]}(q, q') &= (q_\mu - q'_\mu) \mathbf{T}_{\alpha\gamma}(q, -m_V^2) \mathbf{T}_{\gamma\beta}(q', -m_V^2), \\ T_{\mu\alpha\beta}^{[2]}(q, q') &= \mathbf{T}_{\mu\alpha}(q, -m_V^2) \mathbf{T}_{\beta\delta}(q', -m_V^2) q_\delta \\ & \quad - \mathbf{T}_{\mu\beta}(q', -m_V^2) \mathbf{T}_{\alpha\delta}(q, -m_V^2) q'_\delta, \quad (2.40) \\ T_{\mu\alpha\beta}^{[3]}(q, q') &= \frac{q_\mu - q'_\mu}{2m_V^2} \mathbf{T}_{\alpha\gamma}(q, -m_V^2) q'_\gamma \mathbf{T}_{\beta\delta}(q', -m_V^2) q_\delta, \end{aligned}$$

m_V is the mass of the vector meson, and

$$\mathbf{T}_{\alpha\beta}(q, -m_V^2) = \delta_{\alpha\beta} + \frac{q_\alpha q_\beta}{m_V^2}. \quad (2.41)$$

One can construct a set of tensors $O_{\mu\alpha\beta}^{[i]}$ which can be used to project out from $\Lambda_{\mu\alpha\beta}(q, q')$ each of the form factors in Eq. (2.39); i.e., $G_i(Q^2) = O_{\mu\alpha\beta}^{[i]} \Lambda_{\mu\alpha\beta}(q, q')$.

Alternatively, one may construct from linear combinations of the tensors in Eqs. (2.40) a set of tensors that transform irreducibly under spatial rotations in a frame where there is no energy transferred to the final ρ meson, so $Q_\mu = (\vec{Q}, 0)$. The form factors associated with this set of tensors are the electric monopole $G_E(Q^2)$, magnetic dipole $G_M(Q^2)$, and electric quadrupole $G_Q(Q^2)$ form factors. They are related to the original set of form factors by

$$\begin{aligned} G_E(Q^2) &= G_1(Q^2) + \frac{2}{3} \frac{Q^2}{4m_V^2} G_Q(Q^2), \\ G_M(Q^2) &= -G_2(Q^2), \\ G_Q(Q^2) &= G_1(Q^2) + G_2(Q^2) + \left(1 + \frac{Q^2}{4m_V^2}\right) G_3(Q^2). \end{aligned} \quad (2.42)$$

Similarly, one can construct three tensors that project out these form factors from the transition amplitude in an obvious manner, so that $G_E(Q^2) = O_{\mu\alpha\beta}^{[E]} \Lambda_{\mu\alpha\beta}(q, q')$.

The amplitude $\Lambda_{\mu\alpha\beta}(q, q')$ receives contributions from many different sources. The electromagnetic properties of the vector meson arise from both its quark substructure as well as from its mixings with other hadron states, such as two-pion intermediate states. The quark-antiquark contribution to the vector-meson EM form factors was explored in Ref. [5] using the same dynamical

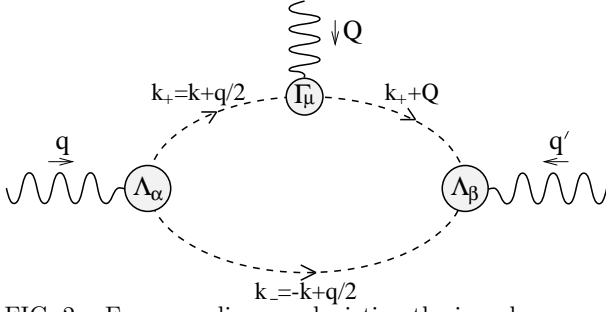


FIG. 2. Feynman diagram depicting the impulse approximate two-pion loop contribution to the ρ -meson electromagnetic transition amplitude $\Lambda_{\mu\alpha\beta}(p, p')$ of Eq. (2.43).

model described in Sec. IV. The EM form factors that arise from the *quark-antiquark* substructure of the vector meson are denoted herein as $G_i^{q\bar{q}}(Q^2)$. This present study extends the work of Ref. [5] by exploring the extent to which π -meson loops contribute to the ρ -meson EM form factors, denoted $G_i^{\pi\pi}(Q^2)$, and ρ -meson charge radius.

In impulse approximation, the two-pion loop contribution to the ρ -meson EM transition amplitude is illustrated in Fig. 2 and is given by

$$\Lambda_{\mu\alpha\beta}(q, q') = -4i \int \frac{d^4k}{(2\pi)^4} \Delta(k_+) \Gamma_\mu(k_+ + \frac{1}{2}Q; Q) \times \Delta(k_+ + Q) \Lambda_\beta^{3-+}(k_+ + Q, k_-) \Delta(k_-) \Lambda_\alpha^{3+-}(k_-, k_+), \quad (2.43)$$

where $k_\pm = \frac{1}{2}q \pm k$, and the Λ_μ^{ijk} are as defined in Eq. (2.3). Isospin invariance entails that the photon couples only to the charged π meson in the above π -loop integration.

The π -meson EM transition amplitude, given in terms of the usual pion EM form factor, is

$$\Gamma_\mu(k_+ + \frac{1}{2}Q; Q) = 2(k_+ + \frac{1}{2}Q)_\mu F_\pi(Q^2), \quad (2.44)$$

where $k_+ + \frac{1}{2}Q$ is the average momentum of the incoming and outgoing pions, and $Q = -q - q'$ is the momentum transferred to the final vector meson by the photon.

Substituting the relation in Eq. (2.44) into Eq. (2.43), one obtains

$$\Lambda_{\mu\alpha\beta}(q, q') = 8ig_{\rho\pi\pi}^2 \int \frac{d^4k}{(2\pi)^4} \Delta(k_+) (k_+ + \frac{1}{2}Q)_\mu F_\pi(Q^2) \times \Delta(k_+ + Q) k_\alpha f^{VPP}(k_-, k_+) \Delta(k_-) \times (k_+ + \frac{1}{2}Q)_\beta f^{VPP}(k_+ + Q, k_-). \quad (2.45)$$

As in the case of the vector meson self-energy $\Pi_{\mu\nu}(q)$, the π -meson loop integration in Eq. (2.45) necessarily samples momenta for which *both* pions are on-mass-shell when $q^2 = q'^2 = -m_\rho^2$. It follows that ρ -meson EM form factors are, in general, complex functions of Q^2 .

The imaginary parts of these form factors are associated with interference between the *photo-stimulated* decay of the ρ meson into two pions and the usual decay

of the ρ meson into two pions. The real parts of the EM form factors correspond to the situation where the intermediate mesons remain off-mass-shell. Hence, they are not observed as an asymptotic state and the ρ meson remains intact. The real parts of the EM form factors are associated with the charge distribution of the ρ meson. Thus, only the real parts of the ρ -meson electromagnetic form factors are of interest to the present study.

As in the previous calculation of the vector-meson self energy $\Pi_{\mu\nu}(q^2)$, a Feynman parametrization is introduced, thereby combining the three denominators of the pion propagators in Eq. (2.45) into a single denominator,

$$\Delta(k_+) \Delta(k_+ - Q) \Delta(k_-) = \frac{1}{2} \int_{-1}^{+1} d\alpha_1 d\alpha_2 \left[k^2 + m_\pi^2 + \frac{q^2}{4} - \alpha_1 k \cdot q - (\alpha_1 + \alpha_2)(k \cdot Q + \frac{1}{2}q \cdot Q + \frac{1}{2}Q^2) \right]^{-3}. \quad (2.46)$$

The EM form factors of the vector meson are Lorentz invariant and can be calculated in any frame. Herein, the calculation is performed in the Breit frame for which $Q_\mu = (0, 0, Q, 0)$ and $q_\mu = (0, 0, -\frac{1}{2}Q, i\sqrt{\frac{1}{4}Q^2 + m_\rho^2})$, $k \cdot Q = x\sqrt{1-z^2}\sqrt{k^2Q^2}$, $k \cdot q = -\frac{1}{2}k \cdot Q + iz\sqrt{k^2(\frac{1}{4}Q^2 + m_\rho^2)}$, and the elastic condition $2Q \cdot q = -Q^2$ is satisfied. Then using the projection operators $O_{\mu\alpha\beta}^{[i]}$ discussed above and translating the k^2 -integration domain by

$$k \rightarrow \tilde{k} = k + \frac{1}{2}\alpha_1 q + \frac{1}{2}(\alpha_1 + \alpha_2)Q, \quad (2.47)$$

one finds that the two-pion contribution to the ρ -meson EM form factor is given by

$$G_i^{\pi\pi}(Q^2) = \frac{2i}{(2\pi)^3} \int_0^\infty k^2 dk^2 \int_{-1}^{+1} \sqrt{1-z^2} dz dx d\alpha_1 d\alpha_2 \times \frac{\mathcal{F}^i}{[k^2 - k_0^2 - i\epsilon]^3}, \quad (2.48)$$

where

$$k_0^2 = -\frac{1}{4}(1-\alpha_1^2)q^2 - m_\pi^2 + \frac{1}{4}(\alpha_1 + \alpha_2)(\alpha_2 + 1)Q^2, \quad (2.49)$$

$$\mathcal{F}^i = O_{\mu\alpha\beta}^{[i]} \left[k + \frac{1}{2}(\alpha_1 + 1)q + \frac{1}{2}(\alpha_1 + \alpha_2 + 1)Q \right]_\mu k'_\alpha k''_\beta \times F_\pi(Q^2) g_{\rho\pi\pi}^2 f^{VPP}(\tilde{k}_-, \tilde{k}_+) f^{VPP}(\tilde{k}_+ + Q, \tilde{k}_-) \quad (2.50)$$

$$k' = k + \frac{1}{2}\alpha_1 q + \frac{1}{2}(\alpha_1 + \alpha_2)Q, \quad (2.51)$$

$$k'' = k' + \frac{1}{2}Q \quad (2.52)$$

$$\tilde{k}_\pm = \pm \left[k + \frac{1}{2}\alpha_1 q + \frac{1}{2}(\alpha_1 + \alpha_2)Q \right] + \frac{1}{2}q. \quad (2.53)$$

Performing the k integration by parts twice, Eq. (2.48) yields

$$G_i^{\pi\pi}(Q^2) = \frac{i}{(2\pi)^3} \int_{-1}^{+1} \sqrt{1-z^2} dz dx d\alpha_1 d\alpha_2 \times \left(\int_0^\infty dk^2 \frac{1}{[k^2 - k_0^2 - i\epsilon]} \left[\frac{\partial}{\partial k^2} \right]^2 k^2 \mathcal{F}^i - \frac{\mathcal{F}^i}{k_0^2} \Big|_{k^2=0} \right). \quad (2.54)$$

The *real* part of this amplitude is of interest, which is obtained from the principal parts of the integrations. As in the calculation of the vector-meson self energy $\Pi_{\mu\nu}(q)$ described in previous sections, calculation of the real part of such amplitude requires a knowledge of the off-mass-shell transition form factor $f^{VPP}(p_1, p_2)$ appearing in \mathcal{F}^i . This is the same form factor that appears in Eq. (2.25) for the calculation of the vector-meson self energy $\Pi^{PP}(q^2)$. The determination of this form factor is carried out in Sec. IV, and the results of numerical calculations of the ρ -meson EM form factors will be postponed until Sec. V. However, it is important to note that the fact that $f^{VPP}(p_1, p_2)$ appears in the calculations of both $\Pi_{\mu\nu}(q)$ and $G_E(Q^2)$ provides a self-consistency check of the dynamical model for $f^{VPP}(p_1, p_2)$. For a dynamical model to be acceptable, it must lead to an off-mass-shell transition form factor $f^{VPP}(p_1, p_2)$ that when substituted into Eqs. (2.24) and (2.48) gives reasonable results for both the ρ - ω mass splitting and the ρ -meson electromagnetic form factor. This issue is discussed further in Sec. V.

Since the ρ -meson EM form factor receives contributions from its quark substructure as well as from meson loops, the ρ meson electric-monopole form factor is written as the sum:

$$G_E(Q^2) = \frac{G_E^{q\bar{q}}(Q^2) + G_E^{\pi\pi}(Q^2)}{G_E^{q\bar{q}}(0) + G_E^{\pi\pi}(0)}. \quad (2.55)$$

Here, the factors in the denominator ensure the unit charge of the ρ meson $G_E(0) = 1$.

In Ref. [5], it was noted that the quark-photon vertex obeys the Ward identity which results from the $U(1)$ -gauge invariance of QED. When quark-photon vertex satisfies this identity and the Bethe-Salpeter amplitudes for the ρ meson are normalized in the canonical manner, the charge conservation condition [$G_E^{q\bar{q}}(0) = 1$] for the ρ meson is guaranteed. A similar Ward identity constrains the behavior of the pion-photon vertex,

$$\lim_{Q \rightarrow 0} \Gamma_\mu(p, p - Q) = \frac{d}{dp_\mu} \Delta^{-1}(p). \quad (2.56)$$

This identity is satisfied by the form introduced in Eq. (2.44). It is straight-forward to show that this identity provides a relation between the magnitude of the form factor $G_E^{\pi\pi}(0)$ and the derivative of the self energy $\Pi^{PP}(-m_\rho^2, m_\pi, m_\pi)$. This is done by examining the amplitude $\Lambda_{\mu\alpha\beta}(q, q')$ of Eq. (2.45) in the limit that the photon momentum $Q \rightarrow 0$. Then, with the identity in Eq. (2.56), one can show that

$$\begin{aligned} \lim_{Q \rightarrow 0} O_{\mu\alpha\beta}^{[E]} \Lambda_{\mu\alpha\beta}(q, Q - q) \\ = O_{\mu\alpha\beta}^{[E]} 2q_\mu \mathbf{T}_{\alpha\beta}(q, -m_\rho^2) \left(\frac{d}{dq^2} \Pi^{PP}(q^2, m_\pi, m_\pi) \right)_{q^2 = -m_\rho^2}, \\ = \delta Z_{\pi\pi}, \end{aligned}$$

where $\delta Z_{\pi\pi}$ is that part of the contribution to the normalization of the ρ meson that arises from the two-pion intermediate state:

$$\delta Z_{\pi\pi} = \left(\frac{d}{dq^2} \Pi^{PP}(q^2, m_\pi, m_\pi) \right)_{q^2 = -m_\rho^2}. \quad (2.57)$$

It follows immediately that $G_E^{\pi\pi}(0) = \delta Z_{\pi\pi}$, which is the justification of the choice of normalizations in Eq. (2.55).

From Eq. (2.55), one may calculate the ρ meson EM charge radius in the usual manner,

$$\langle r^2 \rangle = -6 \frac{d}{dQ^2} G_E(Q^2) \quad (2.58)$$

$$= \frac{-6}{1 + G_E^{\pi\pi}(0)} \left(\frac{d}{dQ^2} G_E^{q\bar{q}}(Q^2) + \frac{d}{dQ^2} G_E^{\pi\pi}(Q^2) \right). \quad (2.59)$$

The charge radius that results from a numerical calculation of Eq. (2.59) using Eq. (2.54) is given in Sec. V.

III. APPROXIMATE REDUCTION TO TIME-ORDERED CONTRIBUTIONS

The approach to evaluating the meson-loop corrections to the ρ - ω mass splitting used here is to evaluate the covariant Feynman diagram of Fig. 1, which includes all possible time orderings of the vertices and intermediate meson propagators. This is in contrast with the work of Ref. [3], which evaluates the mass splitting using time-ordered perturbation theory (TOPT), keeping only that part of the Feynman diagram corresponding to two mesons propagating forward in time (the forward-forward time ordering). In TOPT there is a separate contribution from the two-meson Z graph, where the vertices are ordered in such a way that the initial process (for, say, the ρ self energy due to two-pion loops) is the creation of $\rho\pi\pi$ from the vacuum, which then propagate forward in time with the original ρ meson until the original ρ meson annihilates with the two π mesons. This is the backward-backward time ordering. A calculation of the forward time ordering requires knowledge of the $\rho\pi\pi$ vertex at and near the vicinity of the real decay kinematics, where it is reasonably well known. However, a calculation of the backward time ordering requires knowledge of the vertex for the vacuum to $\rho\pi\pi$ process, which is not well known. Fortunately, the vertex for $\rho\pi\pi$ creation and annihilation is believed to be strongly suppressed, and the backward-backward diagram is further suppressed by the energy denominators of the $\rho\rho\pi\pi$ intermediate state propagation. For these reasons, the Z-diagram contribution is excluded from the calculation described in Ref. [3].

With the belief that the multiple-hadron creation and annihilation vertices should suppress the backward-backward time-ordered diagrams, a simple calculation is undertaken to assess the relative importance of this diagram to the forward-forward time ordering in the

present covariant framework. One might argue that predictions obtained within this covariant framework would be neither robust nor reliable if the forward-forward and backward-backward contributions were both large, but of opposite sign and canceled each other. Such subtle cancellations would be very sensitive to details of the model which may not be constrained accurately enough to be trusted. If there were a cancellation between the forward-forward and backward-backward diagrams in the present framework, it could explain the discrepancy between the small vector-meson mass shift obtained herein, and the larger mass shifts obtained in the study of Ref. [3], which keeps only the forward-forward contributions.

To determine the relative importance of the various time-ordered contributions, one starts with the expression in Eq. (2.24), and then rewrites the ρ -meson self energy as a sum of four contributions arising from the four possible time orderings of the two pion propagators. One of these terms is identified with the contribution to the self energy due to the propagation of two *forward-propagating* (positive-energy) pions. The analytic structure and physical interpretation of this term, which is analogous to that calculated in Ref. [3], and the three other terms is discussed in detail. In Sec. V C, a direct numerical evaluation of these terms will show that for time-like values of the vector-meson four momentum q , the dominant contribution to the self energy $\Pi^{PP}(q^2)$ comes from the term identified with the propagation of two forward-propagating pions. Therefore, although the inclusion of *all* four time orderings is necessary to maintain the Lorentz covariance of the present framework, the additional time-orderings present in covariant expressions like Eq. (2.24), are *not* responsible for the significant discrepancy between the mass shifts obtained herein (to be presented in Sec. V C) and those obtained by Ref. [3]. Rather, in the present quantum field theoretic framework, one observes that the term in vector-meson self energy that arises from two forward-propagating pions is, in fact, the dominant contribution.

Before proceeding further, it is necessary to clarify some issues concerning the use of quantum field theoretic models formulated in Euclidean space. In the present study, observables are obtained by analytically continuing the arguments of the Schwinger functions (Euclidean Green functions) into Minkowski space. In principal, this is done by first integrating over the *internal* momenta so that the Schwinger function depends only on Lorentz-scalar products of the external momenta. The Schwinger function can then be analytically continued in these scalar products into Minkowski space. For example, once the integration over the internal momenta k is carried out in Eq. (2.24), the resulting Schwinger function $\Pi^{PP}(q^2)$ depends only on the square of the vector-meson four momentum q^2 . The Schwinger function is then analytically continued into Minkowski space by let-

ting $q^2 \rightarrow -m_\rho^2$.^{*} In the present study, the use of model forms for the elementary Schwinger functions (e.g., quark propagators, Bethe-Salpeter amplitudes and meson transition vertices) allows the analytic continuation of external momenta to be performed in a straight-forward manner by letting external momenta become complex before the internal momenta are integrated over.

An important ramification of such a framework is that a direct comparison between the elementary Schwinger functions employed herein and those employed in other models formulated in Minkowski space is impossible. One reason for this is that the model form of the quark propagators $S_f(k)$, given by Eqs. (4.5), are parametrized in terms of *entire* functions of k . This parametrization provides the model with quark confinement by ensuring that the quark propagator $S_f(k)$ is free of singularities in the finite, complex- k plane. Hence, the quark propagator has no Lehman representation and no quark-production thresholds can arise from the calculation of observables. Of course, the use of such quark propagators also forbids the possibility of performing a Wick rotation in the loop-integration variable k . Therefore, the elementary Schwinger functions employed herein are permanently embedded in Euclidean space. Only final quantities, such as $\Pi^{PP}(q^2)$, can be analytically continued into Minkowski space.

Another feature of the framework that makes a Wick rotation impossible to perform is the rich analytic structure of the meson transition vertices, e.g., $\Lambda_\mu^{ijk}(p, p')$. A Wick rotation of these transition vertices, although possible in principal, is made difficult by the presence of singularities which arise from the many-particle nature of the field theory. In general, these singularities may cross the integration path requiring that exceptional care be taken when performing a Wick rotation. In practice, these transition vertices are calculated and parametrized only on the small domain of the complex-momentum plane for which they are needed in pion-loop integrations; their behavior outside this domain is unknown. Such difficulties are not present in a quantum mechanical formulation that truncates the Fock space in such a way as to include only states with a small number of particles. The analytic properties of transition vertices obtained in such models are more easily analyzed.

Nevertheless, it is possible to make a simple connection between this field theoretic approach and TOPT. The starting point is the calculation of the ρ -meson self energy due to the two-pion loop from Eq. (2.24). As in Ref. [3], the calculation is carried out in the rest frame of the ρ meson. In this frame, $q_\mu = (\vec{0}, im_\rho)$ and the π -meson propagators, which depend on the momenta $k_\pm = k \pm \frac{1}{2}q$,

^{*} Additional details concerning the formulation of quantum field theory in Euclidean space and the analytic properties of Schwinger functions may be found in Ref. [12].

can be written in the following form

$$\Delta(k_{\pm}, m_{\pi}) = \frac{-1}{(ik_4 \mp \frac{1}{2}m_{\rho})^2 - (\omega(\vec{k}^2) - i\epsilon)^2}, \quad (3.1)$$

where $\omega(\vec{k}^2) = \sqrt{\vec{k}^2 + m_{\pi}^2}$. The denominator of Eq. (3.1) is the difference of two squares. It can be factorized and rewritten as a difference of two poles in the complex- k_4 plane,

$$\Delta(k_{\pm}^2, m_{\pi}) = \frac{1}{2\omega(\vec{k}^2)} \left[\frac{1}{ik_4 \mp \frac{1}{2}m_{\rho} + \omega(\vec{k}^2) - i\epsilon} - \frac{1}{ik_4 \mp \frac{1}{2}m_{\rho} - \omega(\vec{k}^2) + i\epsilon} \right]. \quad (3.2)$$

In a field theory based in Minkowski space, the two terms in Eq. (3.2) would be identified with forward- and backward-propagating pions. A similar identification is possible for the two-pion system in our approach by substituting Eq. (3.2) into Eq. (2.24). One then obtains an expression for the vector meson self energy in which four poles in the complex- k_4 plane are explicit. Writing the self energy as a sum of four terms: $\Pi^{PP}(q^2) = \Pi^{[++]}(q^2) + \Pi^{[--]}(q^2) + \Pi^{[+-]}(q^2) + \Pi^{[-+]}(q^2)$, where, for $a, b = +, -$, one has

$$\Pi^{[ab]}(-m_{\rho}^2) = -\frac{4}{3} \int \frac{d^4k}{(2\pi)^4} \frac{\mathcal{F}^{PP}(k, q)}{4\omega^2(\vec{k}^2)} A^{[ab]}(k), \quad (3.3)$$

and

$$A^{[++]}(k) = \left(\frac{1}{ik_4 - \frac{1}{2}m_{\rho} + \omega(\vec{k}^2) - i\epsilon} \right) \times \left(\frac{-1}{ik_4 + \frac{1}{2}m_{\rho} - \omega(\vec{k}^2) + i\epsilon} \right), \quad (3.4)$$

$$A^{[--]}(k) = \left(\frac{-1}{ik_4 - \frac{1}{2}m_{\rho} - \omega(\vec{k}^2) + i\epsilon} \right) \times \left(\frac{1}{ik_4 + \frac{1}{2}m_{\rho} + \omega(\vec{k}^2) - i\epsilon} \right), \quad (3.5)$$

$$A^{[+-]}(k) = \left(\frac{1}{ik_4 - \frac{1}{2}m_{\rho} + \omega(\vec{k}^2) - i\epsilon} \right) \times \left(\frac{1}{ik_4 + \frac{1}{2}m_{\rho} + \omega(\vec{k}^2) - i\epsilon} \right), \quad (3.6)$$

$$A^{[-+]}(k) = \left(\frac{1}{ik_4 - \frac{1}{2}m_{\rho} - \omega(\vec{k}^2) + i\epsilon} \right) \times \left(\frac{1}{ik_4 + \frac{1}{2}m_{\rho} - \omega(\vec{k}^2) + i\epsilon} \right). \quad (3.7)$$

These are identified as contributions to the ρ -meson self energy due to forward-forward ($++$), backward-backward ($--$), forward-backward ($+-$) and backward-forward ($-+$) propagation of the two pions, respectively.

This nomenclature specifies the four possible time orderings of the two pions in the pion loops. It is justified from an analysis of the motion of the poles in the complex- k_4 plane as the three-momentum \vec{k} is varied.

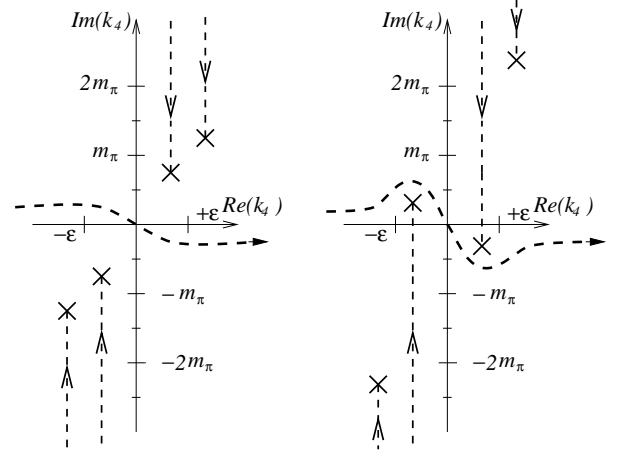


FIG. 3. The positions in the complex- k_4 plane of the poles in Eq. (3.3). Dashed lines with arrows indicate the motion of these poles as the relative three-momentum $|\vec{k}|$ is decreased from infinity to zero. The positions of the poles for $|\vec{k}| = 0$ are denoted by “X.” The diagram on the left depicts the fictional situation for which $m_{\rho} \approx m_{\pi}/2 < 2m_{\pi}$ and the $\rho \rightarrow \pi\pi$ decay is forbidden by energy conservation. The diagram on the right depicts the situation for which $m_{\rho} > 2m_{\pi}$, and the $\rho \rightarrow \pi\pi$ decay is allowed. For a certain values of $|\vec{k}|$, two of the pion poles may pinch the k_4 -contour integration as $\epsilon \rightarrow 0$. This signals the threshold of the $\rho \rightarrow \pi\pi$ decay and results in a cut in the self energy of the ρ meson. These two poles correspond to the forward-forward time ordering in Eq. (3.4).

These integrands in Eq. (3.3) exhibit poles for particular values of the fourth component of the loop-integration momentum k_4 . The positions of these poles depend on the magnitude of the three-momentum \vec{k} as well as the mass of the vector meson m_{ρ} . In Fig. 3, the positions of these poles, along with their motions as $|\vec{k}|$ is varied, are depicted for two possible scenarios. The left diagram corresponds to a scenario (not realized in nature) for which the ρ -meson mass $m_{\rho} \approx m_{\pi}/2 < 2m_{\pi}$. In this situation, the center-of-momentum energy of the ρ meson is below the two-pion decay threshold; hence, the ρ meson is stable with respect to the strong decay into two pions. The diagram on the right depicts the situation (realized in nature) for which the mass of the ρ meson $m_{\rho} > 2m_{\pi}$ and the strong, $\rho \rightarrow \pi\pi$ decay is allowed. In both diagrams, the motions of these poles as $|\vec{k}|$ is varied are denoted by dashed lines. Arrows depict the trajectory of the poles as $|\vec{k}|$ is decreased from infinity to zero. The positions of the poles for $|\vec{k}| = 0$ are denoted by “X.”

Examination of the left diagram in Fig. 3 depicts the fictional situation where the ρ -meson mass is below the $\rho \rightarrow \pi\pi$ threshold energy. Hence, the integrations over

k_4 in Eq. (3.3) never encounter poles for any value of $|\vec{k}|$. Thus, in this scenario, the ρ -meson self energy $\Pi^{PP}(q^2)$ is purely real and the ρ meson is stable with respect to strong interactions. In the right diagram of Fig. 3 for which $m_\rho > 2m_\pi$, one observes a very different situation. Here, as the relative momentum $|\vec{k}|$ is decreased from $-\infty$, two of the poles pass each other, thereby causing the contour integration path for k_4 to become “pinched” in the limit that $\epsilon \rightarrow 0$. Such a pinching of the k_4 -integration contour results in a branch cut in $\Pi^{PP}(q^2)$ and hence a non-zero imaginary part of the vector-meson self energy. This signals the opening of the two-pion decay channel and provides the ρ meson with a finite two-pion decay width. The value of $|\vec{k}|$ for which this pinch first develops is obtained from the energy-conservation condition: $\omega(\vec{k}^2) = m_\rho/2$. The fact that this pinch singularity in $\Pi^{PP}(q^2)$ can only arise in the calculation of $\Pi_{++}(q^2)$ is the justification for this term being identified with the propagation of two forward-propagating pions. Clearly, only positive-energy pions may appear in asymptotically free states and in so doing contribute to the imaginary part of the vector-meson self energy.

The term $\Pi^{--}(q^2)$ is identified as arising from two-backward propagating pions by noting that had one started with the convention that energies were negative rather than positive quantities, the replacement of the ρ -meson center-of-momentum energy m_ρ with $-m_\rho$, would result in the pinch singularity appearing in $\Pi^{--}(q^2)$ rather than in $\Pi^{++}(q^2)$. That is, within a framework that employed such a convention, the asymptotically free states would necessarily contain negative-energy pions. A corollary that follows from the above argument is that in the limit that $q^2 \rightarrow 0$, no energy flows into the two-pion-loop diagram and there is no difference between the forward-forward and backward-backward time orderings; that is, for a massless vector meson these time orderings contribute equally to its self energy. (This is indeed what is observed numerically, as discussed in Sec. V C.)

It is important to note that the contribution to the vector-meson self energy due to negative energy pions does indeed appear in quantum mechanics, even though there are no negative energy states in the Fock space. By considering the time-ordered Feynman diagram associated with $\Pi^{--}(q^2)$, written so that all particles move in the positive-time direction, one observes that the four-particle Fock state $|\rho\rho\pi\pi\rangle$ has a non-zero overlap with the intermediate particles depicted in the diagram. This state contributes only to the real part of the vector-meson self energy because energy conservation forbids the decay $\rho \rightarrow \rho\pi\pi$.

In a quantum mechanical framework, such as that employed in Ref. [3], Cauchy’s Theorem entails that the mixed, forward-backward (+−) and backward-forward (−+) contributions, are identically zero. However, in the present framework the meson-transition vertex in Eq. (4.9) and quark propagator in Eq. (4.5) have essential singularities at infinity. Therefore, one cannot close the

contour the integration at infinity and use Cauchy’s theorem to show that these terms are zero. Consequently, there is no such constraint on the value of these terms in the present approach, and they will generally be different from zero. A discussion of the physical interpretation of these terms and the role they play in determining the unitarity of the theory is left for future investigations. It is sufficient for the present application to note that in Sec. V C, a direct numerical evaluation of these terms shows them to provide a negligible contribution to the vector-meson self energy. Hence, they have no impact on the results presented herein.

IV. MESON TRANSITION AMPLITUDES

In the previous sections, expressions for the vector-meson self energy and EM form factors were given in terms of meson propagators and meson transition amplitudes. In the following section, these transition amplitudes are given in terms of nonperturbative quark-loop integrations that depend on model Bethe-Salpeter amplitudes and nonperturbatively-dressed quark propagators developed in studies of hadron observables based on the Schwinger-Dyson equations of QCD. A recent review of such studies is provided by Ref. [13].

The imaginary part of the vector-meson self energy is determined by meson transition amplitudes for which all external meson momenta are on-mass-shell. It follows that an experimental determination of decay widths for the vector meson provides only the *on-mass-shell* values of the meson transition amplitudes. In the following, the values of the transition amplitudes when all mesons are on-mass-shell are referred to as *coupling constants*, e.g., $g_{\rho\pi\pi}$.

A determination of the real parts of the vector meson self energy requires calculating the principal part of the integrals in Eqs. (2.24) and (2.28), which sample the k^2 -integration domain for which the intermediate mesons are off-mass-shell. Thus, a calculation of the real parts of the self energy and EM form factors requires knowledge of the meson transition form factors for off-mass-shell values of the intermediate meson momenta. As the real part of the self energy is not directly observable, experiment cannot determine the behavior of the off-mass-shell-meson transition form factors. Nonetheless, experimental observations can provide some guidance in helping to constrain the real parts of self energies and EM form factors. This can be done by looking for observables which are proportional to the *difference* of two self energies. For example, from Eqs. (2.30) and (2.31), it is apparent that the ρ - ω mass splitting provides a measure of the difference of the real parts of the ρ and ω self energies. In Sec. IV, the calculation of off-mass-shell meson transition form factors is discussed.

The VVP and VPP vector-meson transition amplitudes are calculated within a generalized impulse ap-

proximation in which the mesons couple to each other by means of a nonperturbatively-dressed quark loop. In this generalized impulse approximation, the quark propagators and meson Bethe-Salpeter amplitudes are nonperturbatively dressed, but explicit three-body interactions are neglected.

In the following, quark-loop integrations are performed in Euclidean space (where $q^2 > 0$), and final results are analytically continued to Minkowski space by letting the external (timelike) momenta $q^2 \rightarrow -m_V^2$. The Dirac matrices γ_μ employed herein are Hermitian, $\gamma_\mu^\dagger = \gamma_\mu$, and satisfy the anti-commutation relation $\{\gamma_\mu, \gamma_\nu\} = 2\delta_{\mu\nu}$.

The amplitude describing the coupling of a vector meson of momentum $q = -p_1 - p_2$ and two pseudoscalar mesons with momentum p_1 and p_2 is given in impulse approximation by[†],

$$\Lambda_\mu^{ijk}(p_1, p_2) = \text{tr}_{CFD} \int \frac{d^4k}{(2\pi)^4} \mathbf{S}(k_{++}) \lambda_i V_\mu(k + \frac{1}{2}p_2; q) \times \mathbf{S}(k_{--}) \lambda_j \Gamma_P(k - \frac{1}{2}q; p_1) \mathbf{S}(k_{--}) \lambda_k \Gamma_P(k; p_2), \quad (4.1)$$

where $k_{\alpha\beta} = k + \frac{\alpha}{2}q + \frac{\beta}{2}p_2$, λ_i are linear combinations of the Gell-Mann SU(3)-flavor matrices associated with the mesons involved, the trace is over color, flavor and Dirac indices, and $\mathbf{S}(k) = \text{diag}(S_u(k), S_d(k), S_s(k))$ is the quark propagator for u , d and s quarks. It is a 3×3 matrix in the quark-flavor space. In this study, the effects of SU(3)-flavor breaking are neglected, so the quark propagator is diagonal in flavor indices and $S_u(k) = S_d(k) = S_s(k)$. Here $V_\mu(k, k')$ is the vector-meson Bethe-Salpeter amplitude for the ρ or ω mesons, and $\Gamma_P(k; p_1)$ is the Bethe-Salpeter amplitude for the $P = \pi$ or K mesons. The flavor structure of the meson Bethe-Salpeter amplitudes is given explicitly in Eq. (4.1) in terms of the 3×3 Gell-Mann matrices λ_i in the quark-flavor space. The meson transition amplitude $\Lambda_\mu^{ijk}(p_1, p_2)$ is depicted in Fig. 1 as a triangle diagram.

The transition form factor defined by Eq. (2.3) is obtained from Eq. (4.1) by choosing values of the flavor indices i, j and k appropriate for the particular process $V \rightarrow PP$ under consideration, and then contracting the amplitude with an appropriate vector. In the case of $\rho^0 \rightarrow \pi^+\pi^-$, one obtains

$$g_{\rho\pi\pi} f^{VPP}(p_1, p_2) = \frac{(p_1 + p_2)_\mu}{m_V^2 - 4m_P^2} \Lambda_\mu^{3-+}(p_1, p_2), \quad (4.2)$$

where the flavor indices refer to the following linear combinations of Gell-Mann matrices $\lambda_\pm = \frac{1}{\sqrt{2}}(\lambda_1 \pm i\lambda_2)$, which are associated with an isovector meson of good charge. The resulting form factor $f^{VPP}(p_1, p_2)$ is the essential dynamical element necessary to calculate the

real part of the two-pseudoscalar intermediate state contribution to the vector-meson self energy $\Pi^{PP}(q^2)$ from Eq. (2.24).

Transition amplitudes for processes involving strange mesons, such as $\rho \rightarrow K\bar{K}$, are obtained by assuming SU(3)-flavor symmetry is exact, so that $S_s(k) = S_u(k)$ and $\Gamma_K(k; p_1) = \Gamma_\pi(k; p_1)$. From considerations of SU(3)-flavor symmetry, one can show that the left-hand-side of Eq. (4.2) gains an additional factor of $1/\sqrt{2}$ for the process $\rho \rightarrow K\bar{K}$. In particular, for $\rho^+ \rightarrow K^+\bar{K}^0$, the analogous result for Eq. (4.2) would be

$$\frac{g_{\rho\pi\pi}}{\sqrt{2}} f^{VVP}(p_1, p_2) = \frac{(p_1 + p_2)_\mu}{m_V^2 - 4m_P^2} \Lambda_\mu^{3K^-K^0}(p_1, p_2). \quad (4.3)$$

Here, the flavor indices denote the linear combinations of Gell-Mann matrices, $\lambda_{K^-} \equiv \frac{1}{\sqrt{2}}(\lambda_4 - i\lambda_5)$ and $\lambda_{K^0} \equiv \frac{1}{\sqrt{2}}(\lambda_6 + i\lambda_7)$. The additional factor of $1/\sqrt{2}$ that appears in Eq. (4.3) relative to that in Eq. (4.2), is the reason for the factor of $1/2$ that appears as the coefficient of $\Pi^{PP}(q^2, m_K, m_K)$ in Eqs. (2.30) and (2.31).

Similarly, the coupling of two vector mesons of momenta $-(p_1 + p_2)$ and p_1 to a pseudoscalar meson of momentum p_2 is given in the impulse approximation by

$$\Lambda_{\mu\nu}^{ijk}(p_1, p_2) = \text{tr}_{CFD} \int \frac{d^4k}{(2\pi)^4} \mathbf{S}(k_{++}) \lambda_i V_\mu(k + \frac{1}{2}p_2; q) \times \mathbf{S}(k_{--}) \lambda_j V_\nu(k - \frac{1}{2}q; p_1) \mathbf{S}(k_{--}) \lambda_k \Gamma_P(k; p_2). \quad (4.4)$$

The elements appearing in Eq. (4.4) are the same as in Eq. (4.1). No new elements are necessary to obtain the VVP transition amplitude. The form factor $f^{VVP}(p_1, p_2)$ is obtained from Eq. (4.4) using Eq. (2.8) and is the essential dynamical element necessary to calculate the real part of the intermediate vector-pseudoscalar contribution to the vector-meson self energy $\Pi^{VP}(q^2, m_V, m_P)$ from Eq. (2.28).

Here too, the assumption of exact-SU(3)-flavor invariance provides a simple relation between the processes $\rho \rightarrow \omega\pi$, $\rho \rightarrow \rho\eta$, $\rho \rightarrow K^*K$, $\omega \rightarrow \rho\pi$, $\omega \rightarrow \omega\eta$, and $\omega \rightarrow K^*K$. The flavor factors that relate these processes lead to the coefficients appearing in front of the vector-pseudoscalar contributions in Eqs. (2.30) and (2.31).

Evaluation of the quark-loop integrations in Eqs. (4.1) and (4.4) requires knowledge of the u -, d - and s -quark propagators as well as the vector-meson and pseudoscalar-meson Bethe-Salpeter amplitudes. These are taken from phenomenological studies of the electromagnetic form factors and strong and weak decays of pseudoscalar and vector mesons [5,8].

The form of the model, dressed-quark propagators are based on several numerical studies of the quark Schwinger-Dyson equation using a realistic model-gluon propagator [10,11]. In a general covariant gauge, the propagator for a quark of flavor f is written as $S_f(k) = -i\gamma \cdot k \sigma_V^f(k^2) + \sigma_S^f(k^2)$. It is well described by the following parametrization:

[†]The sense of all momenta is such that positive momenta flow *into* vertices.

TABLE I. Confined-quark propagator parameters for u , d , and s quarks from Ref. [5]. An entry of “same” for a meson indicates that the value of the parameter is the same as for the quark flavor with which it is grouped.

f/meson	b_0^f	b_1^f	b_2^f	b_3^f	C_f	m_f [MeV]
u, d	0.131	2.900	0.603	0.185	0	5.1
π	same	same	same	same	0.121	0
ρ, ω	0.044	0.580	same	0.462	0	0
s	0.105	2.900	0.540	0.185	0	130.0
K	0.322	same	same	same	0	0
K^*	0.107	0.870	same	0.092	0	0

$$\begin{aligned}\bar{\sigma}_S^f(x) &= \xi[b_1^f x] \xi[b_3^f x] \left(b_0^f + b_2^f \xi[\Lambda x] \right) \\ &\quad + 2\bar{m}_f \xi[2(x + \bar{m}_f^2)] + C_f e^{-2x}, \\ \bar{\sigma}_V^f(x) &= \frac{2(x + \bar{m}_f^2) - 1 + e^{-2(x + \bar{m}_f^2)}}{2(x + \bar{m}_f^2)^2},\end{aligned}\quad (4.5)$$

where $\xi[x] = (1 - e^{-x})/x$, $x = k^2/\lambda^2$, $\bar{\sigma}_S^f = \lambda\sigma_S^f$, $\bar{\sigma}_V^f = \lambda^2\sigma_V^f$, $\bar{m}_f = m_f/\lambda$, $\lambda = 0.566$ GeV, $\Lambda = 10^{-4}$, and where the b_i^f , C_f and m_f are parameters. Since $\xi[x]$ is an entire function, this dressed-quark propagator has *no* Lehmann representation. The lack of a Lehmann representation for $S_f(k)$ is sufficient to ensure that the quarks are confined, since no quark-production thresholds can appear in the calculation of observables. The quark propagator $S_f(k)$ also reduces to a bare-fermion propagator when its momentum is large and spacelike, in accordance with the asymptotic behavior expected from perturbative QCD (up to logarithmic corrections). The parameters for the u -, d - and s -quark propagators were determined in Ref. [8] by performing a χ^2 fit to a range of π - and K -meson observables. The parameters for the s -quark propagator employed herein were re-fit in Ref. [5], also from a χ^2 fit to K -meson observables, but with the additional constraint that the resulting s -quark propagator more closely resemble that obtained by the numerical study of Ref. [11]. The resulting parameters are given in Table I.

In the chiral limit $m_f \rightarrow 0$, Goldstone’s theorem allows one to obtain the pseudoscalar-meson Bethe-Salpeter amplitude $\Gamma_P(k; P)$ directly from the dressed-quark propagator $S_f(k)$ [11]. For the calculation of infrared transition amplitudes, like those studied herein, it is sufficient to keep only the part of the pseudoscalar Bethe-Salpeter amplitude that is proportional to γ_5 . In this case, the amplitude is given by

$$\Gamma_P(k; P) = \gamma_5 \frac{B_P(k^2)}{N_P}, \quad (4.6)$$

where $B_P(k^2)$ has the same form as $B_f(k^2)$, one of the Lorentz invariants appearing in the quark inverse propagator $S_f^{-1}(k) = i\gamma \cdot k A_f(k^2) + B_f(k^2)$, but with the

parameters given in Table I for $P = \pi$ or K . The π - and K -meson Bethe-Salpeter amplitudes are obtained from Eqs. (4.5) and (4.6) using the parameters from Table I.

In Eq. (4.6), N_P is the on-mass-shell normalization for the $P = \pi$ or K meson, and is determined by the normalization condition:

$$\begin{aligned}1 &= \frac{N_c p_\mu \text{tr}_D}{m_P} \int \frac{d^4 k}{(2\pi)^4} \\ &\quad \frac{d}{dp_\mu} S(k + \tfrac{1}{2}p) \Gamma_P(k; p) S(k - \tfrac{1}{2}p) \bar{\Gamma}_P(k; p) \\ &\quad + S(k + \tfrac{1}{2}p) \Gamma_P(k; p) \frac{d}{dp_\mu} S(k - \tfrac{1}{2}p) \bar{\Gamma}_P(k; p),\end{aligned}\quad (4.7)$$

where tr_D denotes a trace over Dirac indices and $N_c = 3$. In Ref. [11] it was shown that by maintaining only the Dirac amplitude proportional to γ_5 in the pion Bethe-Salpeter amplitude, one cannot reproduce the ultraviolet behavior of the pion electromagnetic form factor. To do so requires the inclusion of the axial-vector $\gamma_5 \gamma \cdot p$ components into the π -meson Bethe-Salpeter amplitude. Nonetheless, for the calculation of observables which involve small momentum transfers, neglecting Dirac moments other than γ_5 and normalizing the Bethe-Salpeter amplitude according to Eq. (4.7) is usually sufficient.

The vector meson Bethe-Salpeter amplitudes employed herein are taken from Ref. [5]:

$$V_\mu(k; p) = \left(\gamma_\mu + \frac{p_\mu \gamma \cdot p}{m_V^2} \right) \frac{B_V(k^2)}{N_V}, \quad (4.8)$$

where p is the momentum of the vector meson with mass m_V , k is the relative momenta of the quark and antiquark, N_V is the Bethe-Salpeter normalization, obtained from an obvious generalization of Eq. (4.7), and $B_V(k^2)$ has the same form as the Lorentz-invariant function $B_f(k^2)$ found from the quark propagator of Eq. (4.5) with parameters given in Table I with $V = \rho, \omega$ or K^* .

Again, all but the leading Dirac moment proportional to γ_μ in the vector meson Bethe-Salpeter amplitude have been neglected. A numerical study [14] of the Bethe-Salpeter equation that employed a separable model for the quark-antiquark scattering kernel found that the magnitude of this moment is about ten times larger than the next largest. However, some observables may be more sensitive to sub-leading Dirac moments in the Bethe-Salpeter amplitude. Indeed, this was the case observed in Ref. [11] for the asymptotic- q^2 behavior of the π meson electromagnetic form factor. However, the simple form provided by Eq. (4.8) is sufficient to provide a reasonable model for calculating the off-mass-shell transition form factors $f^{VPP}(p_1, p_2)$ and $f^{VVP}(p_1, p_2)$.

With these elements having already been determined by previous studies, the on- and off-mass-shell values of the transition amplitudes $\Lambda_\mu^{VPP}(p_1, p_2)$ and $\Lambda_{\mu\nu}^{VVP}(p_1, p_2)$ can be calculated with no adjustable parameters. The value of a transition amplitude for on-mass-shell meson momenta is referred to as a “coupling

constant". If the invariant mass of the final state \sqrt{s} is less than the mass of the initial state, the decay is allowed to proceed and the coupling constant is experimentally observable. If energy conservation prevents all external mesons from being simultaneously on-mass-shell, one can still define the "coupling constant" as the value of the transition amplitude at this point. However, in this case, there is no decay from which it can be measured experimentally.

In Ref. [5], the coupling constants $g_{\rho\pi\pi}$ and $g_{K^*K\pi}$ were obtained using the model quark propagators from Eqs. (4.5) and Bethe-Salpeter amplitudes from Eqs. (4.6) and (4.8) with the parameters from Table I. The values for $g_{\rho\pi\pi}$ and $g_{K^*K\pi}$ obtained therein were 8.52 and 9.66, respectively. The experimentally observed values for these coupling constants are 6.03 ± 0.02 and 6.40 ± 0.04 , respectively. There are several possible reasons that this model gives results for the decay widths of a vector meson into two pseudoscalars that are larger than obtained by experiment. The first is that for this process in particular, higher Dirac moments contribute significantly to the magnitude of the coupling constant [15]. The second is the possibility that final-state interactions may also be important. For these reasons, rather than employ the value of $g_{\rho\pi\pi}$ obtained in Ref. [5], the experimentally determined value of $g_{\rho\pi\pi} = 6.03$ is used. The meson transition form factors $f^{VPP}(p_1, p_2)$ and $f^{VVP}(p_1, p_2)$ are the important dynamical element necessary for the present calculations. The scales of these are rather insensitive to details of the model Bethe-Salpeter amplitudes, so that the model of Ref. [5] is quite adequate for their determination.

The coupling constant $g_{\rho\omega\pi} = 10.81$ is obtained from the $\rho\omega\pi$ transition amplitude in Eq. (4.4), when all three mesons are on-mass-shell. Of course, the lack of phase space makes the decay $\omega \rightarrow \rho\pi$ impossible, so that the vector-meson self energy contribution due to vector-pseudoscalar intermediate meson states is real for a physical vector meson; i.e., the value of $g_{\rho\omega\pi}$ cannot be determined experimentally. Throughout this article, the value $g_{\rho\omega\pi} = 10.81$ obtained from Eqs. (2.28) with (2.29) is used [16]. For comparison, the value of this coupling constant can be estimated from the anomalous Wess-Zumino term in an effective chiral Lagrangian with the assumption of a universal ρ -meson coupling. With the definition of the coupling constant from Eq. (2.8), it is found to be $g_{\rho\omega\pi} \approx 11.5$ [17], which is consistent with the results of the present calculation. Similarly, a study of the decays of the ω -meson using vector-meson dominance finds the value $g_{\rho\omega\pi} \approx 9.7$ Ref. [18].

The loop integrations of Eqs. (2.24) and (2.28) sample the meson transition form factors $f^{VPP}(p_1, p_2)$ and $f^{VVP}(p_1, p_2)$ for *off-mass-shell* values of the intermediate-meson four momenta p_1 and p_2 . A calculation of these form factors from the quark-loop integrations of Eqs. (4.1) and (4.4) requires a suitable definition for meson Bethe-Salpeter amplitudes when their total momentum is off-mass-shell. Although Bethe-Salpeter

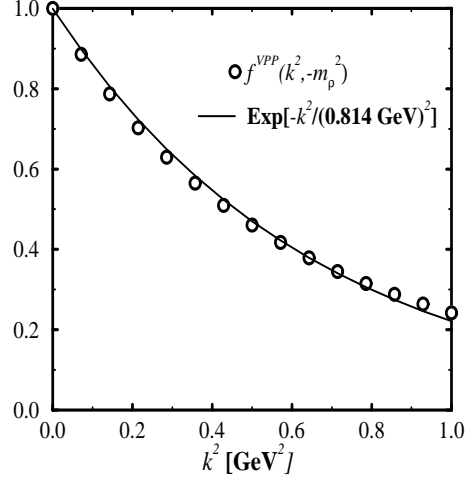


FIG. 4. The meson transition form factor $f^{VPP}(p_1, p_2)$ obtained from Eqs. (4.1) (circles) and the numerical fit (solid curve) of Eq. (4.11) used in the calculations of vector meson self energies and EM form factors.

amplitudes are uniquely determined from the homogeneous Bethe-Salpeter equation for on-mass-shell values of the total momentum, an extrapolation of the amplitude away from this on-mass-shell value is *not* uniquely determined, and hence, is model dependent.

Herein, the Bethe-Salpeter amplitudes as defined in Eqs. (4.6) and (4.8) are used, even for values of the meson four momenta that are off-mass-shell. This is most similar to the procedure employed in quark model calculations such as Ref. [3], where a complete set of intermediate states is inserted between the vector-meson states leading to transition amplitudes for on-shell mesons. The off-shell behavior of the intermediate mesons is then determined solely by the behavior of the meson propagators.

Rather than directly use the numerical values of the meson transition form factors as calculated from Eqs. (4.1) and (4.4), it is found that the resulting form factors can be parametrized in terms of the following functions:

$$f^{VPP}(k + \frac{q}{2}, -k + \frac{q}{2}) = \exp\left(-\frac{k^2 + m_P^2 - \frac{1}{4}m_V^2}{b_{VPP}^2(q^2)}\right), \quad (4.9)$$

$$f^{VVP}(k + \frac{q}{2}, -k + \frac{q}{2}) = \left(\frac{1 - m_P^2/b_{VPP}^2(q^2)}{1 + k^2/b_{VPP}^2(q^2)}\right)^2, \quad (4.10)$$

where $p_1 = \frac{1}{2}q + k$ and $p_2 = \frac{1}{2}q - k$ in Eq. (4.9) and Eq. (4.10). The parameters are chosen by fitting these forms to the numerical results on the domain $k^2 \in (0, 1)$ GeV² for a range of external vector-meson four momenta $q^2 \in (-1, +1)$ GeV². The q^2 -dependence of the resulting parameters is well described in terms of the linear forms:

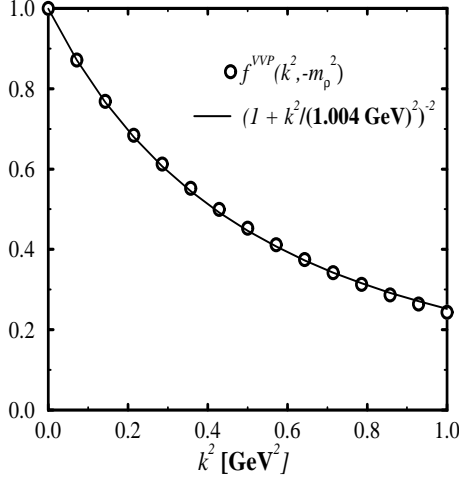


FIG. 5. The meson transition form factor f^{VVP} obtained from Eqs. (4.4) (circles) and the numerical fit (solid curve) of Eq. (4.12) used in the calculations of vector meson self energies.

$$\begin{aligned} b_{VPP}(q^2) &= b_{VPP}^0 + b_{VPP}^1 q^2, \\ b_{VPP}^0 &= 0.855 \text{ GeV}, \\ b_{VPP}^1 &= 0.0693 \text{ GeV}^{-1}, \end{aligned} \quad (4.11)$$

and

$$\begin{aligned} b_{VVP}(q^2) &= b_{VVP}^0 + b_{VVP}^1 q^2, \\ b_{VVP}^0 &= 1.098 \text{ GeV}, \\ b_{VVP}^1 &= 0.159 \text{ GeV}^{-1}. \end{aligned} \quad (4.12)$$

The numerical results (denoted by circles) and the fits (solid curves) are shown in Figs. 4 and 5 for $q^2 = -m_\rho^2$ for the form factors $f^{VPP}(p_1, p_2)$ and $f^{VVP}(p_1, p_2)$, respectively. The similarity of the two curves suggests that both could have just as easily been fitted to either exponential or dipole forms. The choice of one form over the other is arbitrary, and does not affect the results obtained herein.

V. RESULTS AND DISCUSSION

A. mass dependence

Fig. 6 shows the real (solid curves) and imaginary (dashed curves) parts of the contributions to the vector self energy due to $\pi\pi$ and KK loops as a function of the four-momentum squared of the vector meson q^2 . These curves are obtained by calculating $\Pi^{PP}(q^2, m_P, m_P)$ with $P = \pi$ or K in Eqs. (2.24) and (2.25) with the assumption of exact SU(3)-flavor symmetry; i.e., $g_{\rho\pi\pi} = g_{\rho KK} = 6.03$ and using the parametrization of $f^{VPP}(p_1, p_2)$ given by Eq. (4.9).

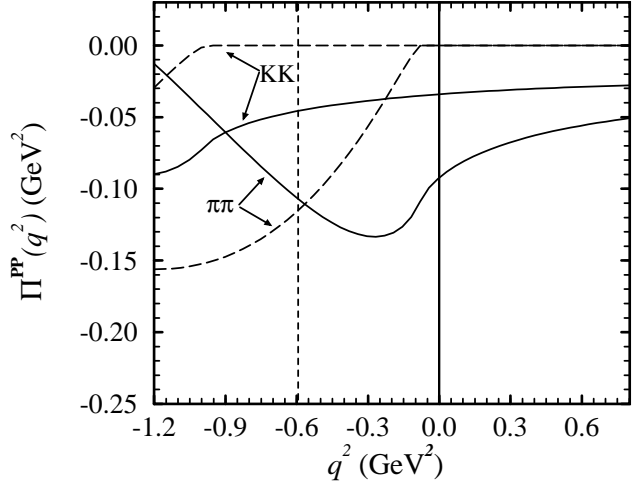


FIG. 6. The real (solid curves) and imaginary (dashed curves) parts of the vector-meson self energy due to intermediate $\pi\pi$ and KK meson states. The vertical dashed line denotes the on-mass-shell point $q^2 = -m_\rho^2$ for the ρ meson and the vertical solid line denotes $q^2 = 0$.

For spacelike values of the vector-meson momenta $q^2 > 0$ (to the right of the solid vertical line in Fig. 6), the self energy $\Pi^{PP}(q^2, m_P, m_P)$ is purely real and approaches zero monotonically from below as $q^2 \rightarrow +\infty$. The threshold for the decay $\rho \rightarrow \pi\pi$ is at $q^2 = -4m_\pi^2$ (just left of the solid vertical line in Fig. 6). Here, the imaginary part of the self energy $\Pi^{PP}(q^2, m_\pi, m_\pi)$ becomes non-zero. This abrupt change of the imaginary part of the self energy at the two-pion threshold leads to a discontinuity in the *second derivative* of the real part of the self energy. This causes the real part of the self energy to rapidly turn over at $q^2 \approx -0.3 \text{ GeV}^2$ and start to approach zero as q^2 becomes more negative (time-like). The same behavior is observed in the two- K -meson self energy $\Pi^{PP}(q^2, m_K, m_K)$, but much deeper in the timelike region since the two-kaon decay threshold is at $q^2 = -4m_K^2 \approx -1 \text{ GeV}^2$.

The discontinuity in the second derivative of $\text{Re}\Pi^{PP}(q^2, m_P, m_P)$ at $q^2 = -4m_P^2$ is a general feature of an amplitude near the threshold of a decay into a two-meson intermediate state with $L = 1$ relative angular momentum. In general, the dependence of the imaginary part of the self energy on the center-of-momentum energy \sqrt{s} near a decay threshold is proportional to $\sqrt{s}^{(1+2L)}$, where L is the relative angular momentum of the two outgoing decay products. The centrifugal barrier due to the relative angular momentum L tends to soften the behavior of the imaginary part of the amplitude at threshold. In the present case of $\rho \rightarrow \pi\pi$, the pions have relative $L = 1$ angular momentum and hence the second derivative of $\text{Re}\Pi^{PP}(q^2, m_P, m_P)$ is discontinuous at $q^2 = -4m_P^2$. Had this two-body decay process proceeded

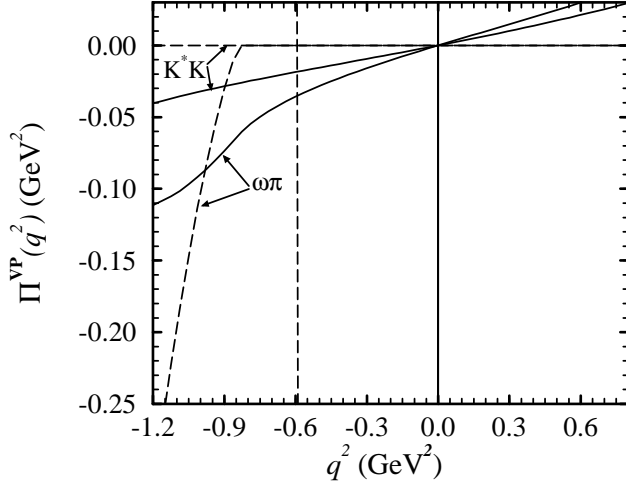


FIG. 7. The real (solid curves) and imaginary (dashed curves) parts of the vector-meson self energy due to intermediate $\omega\pi$ and K^*K meson states. The vertical dashed line denotes the on-mass-shell point $q^2 = -m_\rho^2$ for the ρ meson and the vertical solid line denotes $q^2 = 0$.

in the s -channel with $L = 0$, the *first* derivative of the self energy would have been observed as being discontinuous at threshold $q^2 = -4m_P^2$.

In Fig. 7 the real (solid curves) and imaginary (dashed curves) parts of the vector-meson self energy due to vector-pseudoscalar intermediate state $\Pi^{VP}(q^2, m_V, m_P)$ is shown as a function of q^2 . These curves are obtained by calculating $\Pi^{VP}(q^2, m_V, m_P)$ with $P = \pi$ and $V = \rho$ or $P = K$ and $V = K^*$ in Eqs. (2.28) and (2.29) with the assumption of exact SU(3)-flavor symmetry; i.e., $g_{\rho\omega\pi} = g_{\rho K^*K} = 10.81$ and using the parametrization of $f^{VVP}(p_1, p_2)$ given by Eq. (4.10).

Although not apparent from Fig. 7, when the vector-meson four momentum becomes large and space-like, $q^2 \rightarrow +\infty$, the real part of the self energy $\Pi^{VP}(q^2, m_V, m_P)$ approaches zero from above. The fact that the decay threshold for $\rho \rightarrow \omega\pi$ is observed at $q^2 = -(m_\omega + m_\pi)^2 \approx -0.84 \text{ GeV}^2$, so far above the on-mass-shell value of $q^2 = -m_\rho^2$ means that very little structure for the real part of $\Pi^{VP}(q^2, m_\omega, m_\pi)$ is observed for the range of q^2 plotted in Fig. 7. The lack of structure in the real part of $\Pi^{VP}(q^2, m_{K^*}, m_K)$ for the K^*K channel is even more apparent, owing to the fact that the threshold for $\rho \rightarrow K^*K$ is found at $q^2 = -(m_{K^*} + m_K)^2 \approx -1.9 \text{ GeV}^2$ (not shown in Fig. 7).

As discussed above for $\Pi^{PP}(q^2, m_P, m_P)$, the order in which the discontinuity in derivatives of the real part of the self energy appears is determined by the relative angular momentum L of the out-going decay products. It is straight-forward to show that the decay of a vector meson with $J^P = 1^-$ into a vector and pseudoscalar meson with $J^P = 0^-$ must be in an orbital angular momen-

tum $L = 1$ state. Hence, the discontinuity is expected to appear in the second derivative of $\text{Re}\Pi^{VP}(q^2, m_V, m_P)$ at $q^2 = -(m_\omega + m_\pi)^2$. Numerical differentiation of the results shown in Fig. 7 confirm the presence of this discontinuity.

One observes that $\Pi^{VP}(q^2, m_V, m_P)$ passes through zero at $q^2 = 0$, a feature that is not observed for $\Pi^{PP}(q^2, m_P, m_P)$. This zero is a result of the structure of the VVP meson transition amplitude $\Lambda_{\mu\nu}^{ij}(p_1, p_2)$ given in Eq. (2.8), which is required by Lorentz covariance. The requirement that this amplitude be proportional to

$$\epsilon_{\mu\nu\alpha\beta} p_{1\alpha} p_{2\beta} = \epsilon_{\mu\nu\alpha\beta} q_\alpha p_{1\beta}, \quad (5.1)$$

leads to a vector-meson self energy $\Pi_{\mu\nu}^{VP}(q^2, m_V, m_P)$ that is necessarily transverse to q_μ for all values of q^2 and hence is of the form given in Eq. (2.9). It follows that the vector-meson self energy in this channel vanishes at $q^2 = 0$.

Because the real part of $\Pi_{\mu\nu}^{VP}(q^2, m_V, m_P)$ goes through zero at $q^2 = 0$, approaches zero in the deep spacelike region and is infinitely differentiable below the breakup threshold at $q^2 = -(m_V + m_P)^2$, it is a small and slowly varying function for $q^2 \geq -m_\rho^2$. Therefore, the $\omega\pi^0$ intermediate state is expected to contribute very little to the ρ meson self energy (from Fig. 7, it is clear that the K^*K state contributes even less). However, this channel is important for the self energy of the ω meson, owing to the fact that there are three different $\rho\pi$ channels that contribute to the ω -meson self energy; they are $\rho^+\pi^-$, $\rho^-\pi^+$, and $\rho^0\pi^0$. This leads to the overall factor of three in front of $\Pi_{\mu\nu}^{VP}(q^2, m_\rho, m_\pi)$ in Eq. (2.31), which makes the $\rho\pi$ channel as important for the ω -meson self energy as the $\pi\pi$ channel is for the ρ -meson self energy (see Table II).

A single coupling constant and meson-transition form factors has been used for each of the two types of intermediate states (PP and VP) considered herein. The result is that the only difference between the various channels within a particular type of meson loop is the masses of the intermediate mesons involved. A comparison of the self energies resulting from the KK and K^*K channels with $\pi\pi$ and $\omega\pi$ channels, respectively, suggests that states with heavier mesons contribute less than states of lighter mesons. For example, for all $q^2 \geq -m_\rho^2$, the value of $\Pi^{PP}(q^2, m_K, m_K)$ is less than half the value of $\Pi^{PP}(q^2, m_\pi, m_\pi)$. The same is true when $\Pi^{VP}(q^2, m_{K^*}, m_K)$ is compared with $\Pi^{VP}(q^2, m_\omega, m_\pi)$ in Fig. 7.

Within the present model, the dependence of the vector-meson self energy on the mass of the intermediate mesons can be explored. This is done by letting one or both of the masses m_P in Eqs. (2.24) and (2.28) vary while keeping $q^2 = -m_\rho^2$. The solid curve in Fig. 8 is the result of a calculation of the real part of the self energy $\Pi^{PP}(-m_\rho^2, m_\pi, m_1)$ in which one of the pseudoscalar-meson propagators in Eq. (2.24) has mass m_π and the other propagator has a mass m_1 which is varied from 0

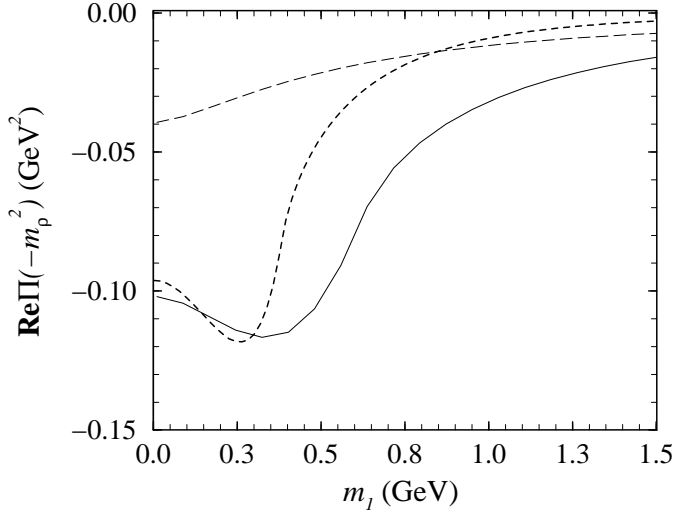


FIG. 8. The dependence of the real part of the vector-meson self energy on the mass m_1 of the intermediate state mesons. The dashed curve shows the dependence of the vector-pseudoscalar channel $\Pi^{VP}(-m_\rho^2, m_\rho, m_1)$ when the mass m_1 of the pseudoscalar meson is varied. The solid curve shows the dependence of the two-pseudoscalar channel $\Pi^{PP}(-m_\rho^2, m_\pi, m_1)$ when the mass m_1 of one of the pseudoscalar mesons is varied. The short-dashed curve shows the dependence of the two-pseudoscalar channel $\Pi^{PP}(-m_\rho^2, m_1, m_1)$ when the mass m_1 of both pseudoscalar mesons is varied.

to 1500 MeV. It is clear from Fig. 8 that the magnitude of the self energy depends critically on the mass m_1 . In particular, for $m_1 = m_\rho$, the real part of the self energy $\Pi^{PP}(-m_\rho^2, m_\pi, m_1)$ has already decreased by a factor of two from its value for $m_1 = m_\pi$. The short-dashed curve in Fig. 8 is the self energy $\Pi^{PP}(-m_\rho^2, m_1, m_1)$ obtained with the masses of the two pseudoscalar mesons are taken to be *equal* and varied together. Increasing both masses of the intermediate mesons at the same time causes the self energy to decrease very rapidly.

It was argued in Ref. [2] that lattice calculations which linearly extrapolate the ρ mass as a function of m_π should receive negligible corrections from the two-pion intermediate state. The calculations described here are in agreement with this conclusion, but as can be seen from the short-dashed curve in Fig. 8, the dependence of the real part of the vector self-energy in the region of the physical pion mass is not smooth, showing the effects of the threshold crossed at $4m_\pi^2$. This rapid dependence on the mass of the intermediate states suggests that such extrapolations must be made with caution.

The dashed curve in Fig. 8 shows the dependence of the self energy $\Pi^{VP}(-m_\rho^2, m_\omega, m_1)$ when the mass of the intermediate vector meson is m_V and the mass of the intermediate pseudoscalar meson m_1 is varied. Because of the different Lorentz-covariant structure of the vector-vector-pseudoscalar transition amplitude $\Lambda_{\mu\nu}^{ij}(p_1, p_2)$ given in

TABLE II. Mass shifts to ρ and ω mesons arising from several two-meson intermediate states. Each channel provides less than a 10% correction to the total mass of the vector meson. The sum of these shifts, which is not observable, is given in the bottom row. The *difference* between these sums is $m_\omega - m_\rho = 24.8$ MeV, which can be compared to the experimental value of 12 ± 1 MeV.

channel	Δm_ρ (MeV)	Δm_ω (MeV)
$\pi\pi$	-69.8	
$K\bar{K}$	-14.8	-14.8
$\omega\pi$	-22.5	
$\rho\pi$		-67.5
$\omega\eta$		-13.1
$\rho\eta$	-13.1	
K^*K	-11.9	-11.9
sum	-132.1	-107.3

Eq. (2.8), and that the threshold for $\rho \rightarrow \omega\pi$ has not been reached even for $m_1 = 0$, a much weaker dependence on the mass m_1 is observed compared to that of $\Pi^{PP}(-m_\rho^2, m_1, m_2)$. Nonetheless, it may be sufficiently accurate to neglect pseudoscalar-vector intermediate states with masses $m_1 \geq m_\rho$ when calculating the self energies, since these are smaller by at least a factor of two than the contribution from the $\omega\pi$ intermediate state.

It is interesting to note that the curves in Fig. 8 all exhibit an extremum for values of m_1 for which the sum of the intermediate-mesons masses ($m_1 + m_2$) is within the range $\frac{1}{2}m_\rho \leq (m_1 + m_2) \leq m_\rho$. This is not coincidental, since m_ρ is the value of the center-of-momentum energy at the decay threshold. For values of $m_1 > m_\rho - m_2$ the real part of the amplitude is a monotonic, decaying function of m_1 . At threshold $m_1 = m_\rho - m_2$, discontinuities in the second derivative of the real part of the self energy cause the rapid turnover observed in Fig. 8, so that the extremum of $\text{Re}\Pi(-m_\rho^2, m_1, m_2)$ occurs for a value of m_1 slightly below the threshold value $m_1 = m_\rho - m_2$.

This suggests that in calculations of self energies for a particle of mass M , it may be sufficiently accurate to consider only those states for which the sum of the intermediate hadron masses $m_1 + m_2 + \dots$ lie on the range $\frac{1}{2}M \leq \sum_i m_i \leq M$. This implies greatly simplified calculations of mixings between states where it is only necessary to consider the contributions from multiple-hadron states within this range of total masses. This is a general feature of such calculations and not a specific result of the particular channels considered herein, since it arises independently of the particular form and scales used to model the meson transition form factors $f^{VPP}(p_1, p_2)$ and $f^{VVP}(p_1, p_2)$.

B. vector-meson mass shifts

Results for the mass shifts due to the two-meson loops considered in this study are summarized in Table II. It should be noted that only the difference between the total mass shifts of the ρ and ω mesons is physically meaningful. The absolute size of each term does, however, give some indication of the importance of the dressing by two-meson loops. The largest mass shifts are that of the ρ mass due to the two-pion loop, and that of the ω due to the $\rho\pi$ loop, which are about -10% of the bare mass.

Note that the ρ mass shift due to the two-pion loop is roughly -70 MeV, while the two-pion ρ mass shift in Ref. [2] was between -10 and -20 MeV. The difference is due to an additional contribution to the vector self-energy which arises from a $\pi\pi\rho\rho$ contact term. This term provides a contribution to the vector-meson self energy $\Pi_{\mu\nu}(q)$ that is independent of q . In Ref. [2], this term is added to provide current conservation for the vector ρ ; i.e., that $\Pi^{PP}(q^2 = 0) = 0$. Since one can show that this term contributes equally to the self energies of the ρ and ω mesons, it cannot contribute to their mass splitting and so has not been included here.

To allow for the direct comparison with Ref. [2], the effects of including this contact term into the present study can be reproduced by subtracting $\Pi(q^2 = 0)$ from the self energy $\Pi(q^2)$. This procedure ensures that the condition obtained in Ref. [2] that $\Pi^{PP}(q^2 = 0) = 0$ is reproduced. The resulting mass shift due to the two-pion loop obtained from Eq. (2.21) would then be approximately

$$\delta m_{\pi\pi} \approx \text{Re} \left[\frac{\Pi^{PP}(-m_\rho^2, m_\pi, m_\pi) - \Pi^{PP}(0, m_\pi, m_\pi)}{2 m_0} \right] \approx -9.2 \text{ MeV}. \quad (5.2)$$

This mass shift for the ρ meson is similar to that of Ref. [2].

As pointed out in Ref. [3], the strange-meson and vector- η intermediate states cannot contribute to the mass splitting; they are included here to illustrate that as the masses of the intermediate state mesons increase, the resulting shifts decrease rapidly. For example, the shift in the ρ mass due to the $K\bar{K}$ intermediate state is about one fifth of that due to two pions. Similarly, the shift in the ω mass due to the $\rho\eta$ intermediate state is roughly half the size of that due to $\omega\pi$.

The result of adding the shifts due to the various intermediate states is that they largely cancel, as in Ref. [3], to give a mass splitting of roughly 25 MeV, which is of the same order (on the scale of the bare mass) as the experimental value of 12 ± 1 MeV. Of course, a complete calculation would have to consider all possible multiple-hadron intermediate states. It is encouraging that, within this model, a reasonable value of the mass splitting is achieved using only a handful of meson loops, and that the individual contributions due to additional loops are expected to be small compared to the dominant contributions evaluated here.

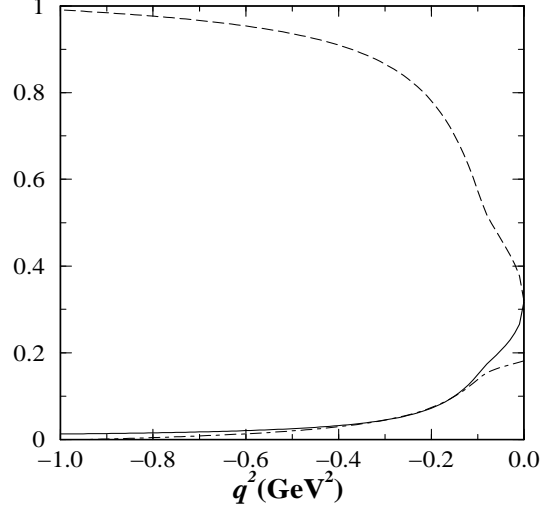


FIG. 9. Ratios of the forward-forward (dashed curve), backward-backward (solid curve) and forward-backward or backward-forward (short-dashed long-dashed curve) time orderings of the real part of the two-pion loop integral to the sum of all four, as a function of the vector-meson mass squared.

C. time orderings

Figure 9 shows the ratio of the forward-forward $\Pi^{[++]}(q^2)$, backward-backward $\Pi^{[--]}(q^2)$, and forward-backward $\Pi^{[+-]}(q^2)$ [equal to backward-forward $\Pi^{[-+]}(q^2)$] time orderings of the real part of the two-pion loop integral to their sum $\Pi^{\pi\pi}(q^2)$, as a function of the vector-meson mass squared q^2 . As expected from the analysis in Sec. III, at $q^2 = 0$ the forward-forward time ordering $\Pi^{[++]}(q^2)$ is equal to the backward-backward time ordering $\Pi^{[--]}(q^2)$. It is also simple to show [by a change of variables from k_4 to $-k_4$ in Eq. 3.3] that $\Pi^{[+-]}(q^2) = \Pi^{[-+]}(q^2)$ at all values of q^2 . Although not shown here, an examination of the derivative of $\Pi^{[++]}(q^2)$ indicates a discontinuity at $q^2 = 4m_\pi^2$ indicating the onset of a branch cut in $\Pi^{\pi\pi}(q^2)$ due to $\Pi^{[++]}(q^2)$, which verifies the identification of this time ordering with the propagation of two forward-propagating pions.

In Fig. 9, one observes that at $q^2 = -m_\rho^2$ the forward-forward time ordering is dominant and the backward-backward contribution is only a few percent of the total. This realizes the expected strong suppression of the backward-backward time ordering, due to the vertices and the large energy denominators for the $\rho\rho\pi\pi$ intermediate state. Note also that both the forward-forward and backward-backward contributions have the same sign, so that the two-pion loop contribution to the ρ self energy is not reduced by a cancellation between these two time orderings. This establishes that, in the present quantum field-theoretic framework, the dominant contribution to the ρ self energy is from two forward-propagating pions,

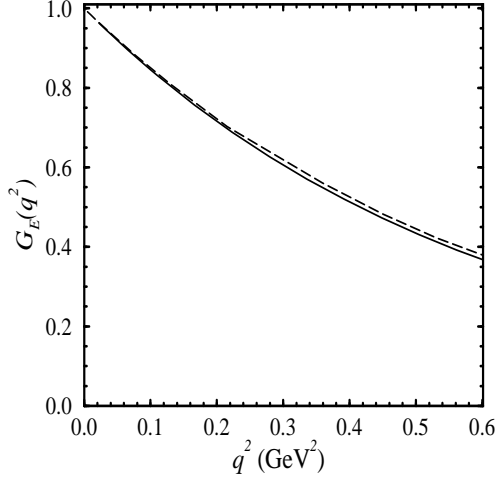


FIG. 10. The ρ -meson electric-monopole form factor. The dashed curve is the result $G_E^{\bar{q}q}(q^2)$ from Ref. [5] that rises from quark-antiquark substructure of ρ meson. The solid curve is the real part of the form factor $G_E(q^2)$ that results when the effects of pion loops from Eq. (2.54) are added to the results from Ref. [5].

and that the difference between the mass shifts obtained in this approach and those of the quantum-mechanical approach of Ref. [3] is not due to the presence of additional time orderings in a Lorentz covariant framework.

As discussed in Sec. 3.3, the forward-backward and backward-forward time orderings are not zero in the present framework; Fig. 9 shows that they also make negligible contributions to $\Pi\pi\pi(q^2)$ at $q^2 = -m_\rho^2$.

D. vector-meson electromagnetic form factors

The final application of vector-meson dressing by two-meson loops that is considered here is the correction to the EM form factors and charge radius of the ρ meson. In Sec. II C, an expression for the pion contribution to the EM form factor $G_i^{\pi\pi}(Q^2)$ was obtained in terms of the same meson transition form factor $f^{VPP}(p_1, p_2)$, given in Eq. (4.9) with Eq. (4.11), that was used to obtain the $\pi\pi$ and $K\bar{K}$ contributions to the ρ -meson self energy.

In the present calculation of $G_E^{\pi\pi}(Q^2)$, the final term in Eq. (2.54) (arising from the surface contribution of the integration by parts) is small and varies slowly with $Q^2 \approx 0$, hence it is safe to neglect this term for the determination of the charge radius. The resulting $G_E^{\pi\pi}(Q^2)$ is well described for spacelike values of the photon momentum squared $0 < Q^2 < 0.8 \text{ GeV}^2$ by the form

$$G_E^{\pi\pi}(Q^2) \approx A e^{-BQ^2/m_\rho^2} \quad (5.3)$$

with $B \approx 1.39$ and the value of A as determined from Eq. (2.57) is $A = \delta Z_{\pi\pi} = 0.134$.

The form factor $G_E^{\pi\pi}(Q^2)$ is added to the quark-antiquark contribution $G_E^{\bar{q}q}(Q^2)$ obtained by Ref. [5] according to Eq. (2.55). The resulting form factor $G_E^{\pi\pi+\bar{q}q}(Q^2)$ is plotted as a solid curve in Fig. 10. It falls more rapidly with the photon momentum Q^2 than does the form factor $G_E^{\bar{q}q}(Q^2)$ (dashed curve) indicating that the inclusion of the $\pi\pi$ intermediate state into the ρ meson self energy has *increased* the charge radius of the ρ meson. The charge radius of the ρ meson due to its quark-antiquark substructure and its mixing with the two-pion state obtained using Eq. (2.59) is

$$\langle r_{q\bar{q}+\pi\pi}^2 \rangle^{\frac{1}{2}} = 0.67 \text{ fm}. \quad (5.4)$$

This value may be compared to the value obtained in Ref. [5],

$$\langle r_{\bar{q}q}^2 \rangle^{\frac{1}{2}} = 0.61 \text{ fm}, \quad (5.5)$$

which results from only the quark-antiquark substructure of the ρ meson. One observes that including pion loops increases the charge radius of the ρ meson by approximately 10%. This is consistent with the increase of less than 15% observed in a similar study of the pion-loop contribution to the π meson charge radius [6].

Although, the short lifetime of the ρ meson excludes the possibility of directly measuring the EM charge radius of the ρ meson at present, one can define a “diffractive radius” from the t dependence of diffractive ρ -meson electroproduction cross sections [7]. As with the EM charge radius, the diffractive radius receives contributions from its quark substructure as well as from mixings with multiple-hadron states. However, an important distinction between the charge radius and the diffractive radius is that since diffraction arises from a strong interaction, electromagnetically neutral particles, such as the ω and ρ^0 mesons, will have diffractive radii even though they have no well-defined charge radius[‡].

The results of this study suggest that the most significant contribution from two-meson loops to the diffractive radius of the ρ meson would be due to the two-pion loop. However, G -parity forbids the ω meson from mixing with the two pions, so that the diffractive radius of the ω meson would be unaffected by the two-pion loop. Therefore, the diffractive radius of the ω meson is expected to be *smaller* than that of the ρ meson. An observed difference in the t -dependence of diffractive electroproduction of ρ and ω mesons would be indicative of their differing diffractive radii, and such a measurement could provide a means to estimate the contributions to these radii from pion loops.

[‡] To be electroproduced diffractively, the vector meson must be able to mix with the photon, and so must be neutral (e.g., ω , ρ^0 , ϕ , J/ψ). Therefore, *only* for neutral vector mesons can one define a diffractive radius.

VI. CONCLUSIONS

It is shown that, in a covariant model based on studies of the Schwinger-Dyson equation of QCD which assumes exact SU(3)-flavor symmetry, the contributions to the self energies of the ρ and ω due to several pseudoscalar-pseudoscalar and pseudoscalar-vector meson loops are at most 10% of the bare mass. The result for the mass shift of the ρ meson due to the two-pion loop is in agreement with a previous calculation of this quantity using an effective chiral Lagrangian approach. Such contributions are found to decrease rapidly as the mass of the intermediate mesons increases beyond $m_\rho/2$.

The mass shifts due to several two-meson intermediate states are compared with those from an extensive study within a nonrelativistic framework of the ρ - ω mass splitting, and are found to be smaller, especially for intermediate states involving higher-mass mesons. A mass splitting of $m_\omega - m_\rho \approx 25$ MeV is found from the $\pi\pi$, $K\bar{K}$, $\omega\pi$, $\rho\pi$, $\omega\eta$, $\rho\eta$ and K^*K channels. A complete calculation which evaluates contributions from all possible multiple hadron intermediate states and breaks SU(3)-flavor symmetry is beyond the scope of the present work. However, these results suggest that such a calculation should exhibit rapid convergence as the number of two-meson intermediate states is increased by including states with higher masses. This implies that inclusion of two-meson loops into the vector-meson self-energy yields a small correction to the predominant valence quark-antiquark structure of the vector meson.

The part of the vector-meson self energy which corresponds to two pions propagating forward in time has been shown to dominate a Lorentz-covariant calculation of the two-pion loop contribution. This implies that the additional time-orderings of this loop, necessary to maintain Lorentz covariance, are not responsible for the reduced size of the mass shifts found in the present framework when compared to quantum-mechanical treatments.

As a test of the self-consistency of this calculation, the contribution of the two-pion loop to the ρ meson EM form factor is evaluated, and is shown to provide a modest increase of about 10% to the charge radius of the ρ . Although this charge radius is difficult to observe, it may be possible to observe the effects of such an increase by examining the difference in the “diffractive radii” of the neutral ρ and ω found from the t -dependence of diffractive electroproduction cross sections. As the two-pion loop cannot contribute to the ω , it may be possible to observe its effects on the ρ by measuring a difference in these diffractive radii.

VII. ACKNOWLEDGMENTS

The authors wish to thank A. Szczepaniak for illuminating discussions. This work is supported by

the U.S. Department of Energy under contracts DE-AC05-84ER40150, DE-FG05-92ER40750 and DE-FG02-87ER40365, and the Florida State University Supercomputer Computations Research Institute which is partially funded by the Department of Energy through contract DE-FC05-85ER25000.

-
- [1] K. L. Mitchell and P. C. Tandy, Phys. Rev. C **55**, 1477 (1995).
 - [2] D. B. Leinweber and T. D. Cohen, Phys. Rev. D **49**, 3512 (1994).
 - [3] P. Geiger and N. Isgur, Phys. Rev. Lett. **67**, 1066 (1991); Phys. Rev. D **41**, 1595 (1990); *ibid* D **44**, 799 (1991).
 - [4] L. C. L. Hollenberg, C. D. Roberts and B. H. J. McKellar, Phys. Rev. C **46**, 2057 (1992).
 - [5] F. T. Hawes and M. A. Pichowsky, Phys. Rev. D **59**, 1743 (1999).
 - [6] R. Alkofer, A. Bender and C. D. Roberts, Int. J. Mod. Phys. A **10**, 3319 (1995).
 - [7] M. A. Pichowsky, “Diffractive radii of hadrons,” in preparation.
 - [8] C. J. Burden, C. D. Roberts and M. J. Thomson, Phys. Lett. B **371**, 163 (1996); C. D. Roberts, Nucl. Phys. A **605**, 475 (1996).
 - [9] M. A. Ivanov, Yu. L. Kalinovsky, P. Maris, and C. D. Roberts, Phys. Rev. C **57**, 1991 (1998); Yu. Kalinovsky, K. L. Mitchell and C. D. Roberts, Phys. Lett. B **399**, 22 (1997); M. A. Pichowsky and T.-S. H. Lee, Phys. Rev. D **56**, 1644 (1997); R. Alkofer, C. D. Roberts, Phys. Lett. B **369**, 101 (1996); M. R. Frank, K. L. Mitchell, C. D. Roberts, P. C. Tandy, Phys. Lett. B **359**, 17 (1995).
 - [10] M. R. Frank and C. D. Roberts, Phys. Rev. C **53**, 390 (1996).
 - [11] P. Maris and C. D. Roberts, Phys. Rev. C **56**, 3369 (1997); P. Maris and C. D. Roberts, Phys. Rev. C **58**, 3659 (1998).
 - [12] C. D. Roberts and A. G. Williams, Prog. Part. Nucl. Phys. **33**, 477 (1994), and references therein.
 - [13] C. D. Roberts, “Nonperturbative QCD with modern tools”, lectures given at the 11th Physics Summer School on Frontiers in Nuclear Physics, Australia National University, Canberra, Australia, LANL e-print # nucl-th/9807026, 1998.
 - [14] C. J. Burden, L. Qian, C. D. Roberts, P. C. Tandy and M. J. Thomson, Phys. Rev. C **55**, 2649 (1997).
 - [15] The importance of including higher Dirac moments in decay processes like $\rho \rightarrow \pi\pi$ was suggested to us by E. S. Swanson, based on quark-model studies of meson decays [see P. Geiger and E. S. Swanson, Phys. Rev. D **50**, 6855 (1994)]. It has since been verified, in calculation of the decay $\rho \rightarrow \pi\pi$ using the model of Ref. [14], that discarding all but the term with the largest strength (proportional to γ_5) in the pion Bethe-Salpeter amplitude tends to increase the coupling constant $g_{\rho\pi\pi}$ by 71% [see

P.C. Tandy, “Modeling nonperturbative QCD for mesons and couplings”, Proceedings of the IVth Workshop on Quantum Chromodynamics, Paris (1998) LANL e-print #nucl-th/9812005].

- [16] In contrast to decays of a vector meson into two pseudoscalar mesons, the transition amplitude of a vector-meson coupling to a vector and pseudoscalar meson is rather insensitive to sub-leading Dirac amplitudes in the meson Bethe-Salpeter amplitudes. Hence, the value for the coupling constant $g_{\omega\rho\pi}$ obtained herein, is more reliable than the result for $g_{\rho\pi\pi}$ obtained in Ref. [5].
- [17] V. Bernard, N. Kaiser and U. G. Meissner, Eur. Phys. J. A **4**, 259 (1999).
- [18] J. W. Durso, Phys. Lett. B **184**, 348 (1987).